Cell Cycle 13:19, 3059–3075; October 1, 2014; © 2014 Taylor & Francis Group, LLC

Different effects of ZO-1, ZO-2 and ZO-3 silencing on kidney collecting duct principal cell proliferation and adhesion

Xiaomu Qiao, Isabelle Roth, Eric Féraille, and Udo Hasler*

Department of Cellular Physiology and Metabolism and Service of Nephrology; University Medical Center; University of Geneva; Geneva, Switzerland

Keywords: adhesion, cell cycle, cyclin D1, kidney collecting duct, proliferation, p21, ZONAB, zonula occludens

Abbreviations: CD, collecting duct; CCD, cortical collecting duct; CycD1, cyclin D1; OMCD, outer medullary collecting duct; PCNA, proliferating cell nuclear antigen; PCT, proximal tubule; TAL, thick ascending limb of Henle's loop; TJ, tight junction; ZO, zonula occludens; ZONAB, ZO-1-associated nucleic acid-binding protein.

Coordinated cell proliferation and ability to form intercellular seals are essential features of epithelial tissue function. Tight junctions (TJs) classically act as paracellular diffusion barriers. More recently, their role in regulating epithelial cell proliferation in conjunction with scaffolding zonula occludens (ZO) proteins has come to light. The kidney collecting duct (CD) is a model of tight epithelium that displays intense proliferation during embryogenesis followed by very low cell turnover in the adult kidney. Here, we examined the influence of each ZO protein (ZO-1, -2 and -3) on CD cell proliferation. We show that all 3 ZO proteins are strongly expressed in native CD and are present at both intercellular junctions and nuclei of cultured CD principal cells ($mCCD_{cl1}$). Suppression of either ZO-1 or ZO-2 resulted in increased G_0/G_1 retention in $mCCD_{cl1}$ cells. ZO-2 suppression decreased cyclin D1 abundance while ZO-1 suppression was accompanied by increased nuclear p21 localization, the depletion of which restored cell cycle progression. Contrary to ZO-1 and ZO-2, ZO-3 expression at intercellular junctions dramatically increased with cell density and relied on the presence of ZO-1. ZO-3 depletion did not affect cell cycle progression but increased cell detachment. This latter event partly relied on increased nuclear cyclin D1 abundance and was associated with altered β1-integrin subcellular distribution and decreased occludin expression at intercellular junctions. These data reveal diverging, but interconnected, roles for each ZO protein in $mCCD_{cl1}$ proliferation. While ZO-1 and ZO-2 participate in cell cycle progression, ZO-3 is an important component of cell adhesion.

Introduction

Tight junctions (TJs) are the most apical component of the intercellular junctional complex that classically function as paracellular diffusion barriers, allowing the partition of distinct apical and basal fluid compartments.[1,2] TJs are multiprotein complexes composed of integral membrane proteins and cytoplasmic scaffolding proteins.[3,4] This latter group includes zonula occludens (ZO) proteins, comprised of ZO-1, -2 and -3, that interact with cytoplasmic domains of transmembrane junctional proteins and participate in determining TJ structural organization.[3,5] ZO proteins also interact with cytosolic proteins, creating higher order molecular structures at junctional sites where various proteins involved in signal transduction and transcriptional modulation are recruited.[6–8] These include proteins involved in epithelial proliferation and differentiation that confer a role for ZOs that goes well beyond their function in regulating paracellular permeability.

By transmitting information about the degree of cell-cell contacts to the nucleus, ZO proteins maintain balance between proliferation and differentiation.[7] ZO-1 influences cell proliferation in part by binding transcription factors that can localize both to adhesion complexes and the nucleus, where they regulate gene expression.[5,9,10] Among these proteins, ZO-1-associated nucleic acid-binding protein (ZONAB) is particularly well described. ZONAB is a Y-box transcription factor that promotes epithelial cell proliferation by inducing expression of cyclin D1 (CycD1) and proliferating cell nuclear antigen (PCNA).[11,12] CycD1 drives G_1-to-S phase transition.[13] By sequestrating ZONAB at junctional sites, and thereby reducing its localization in the nucleus, ZO-1 was shown to reduce cell proliferation.[5,14] Several pieces of data indicate that ZO-2 shuttles numerous proteins in and out of the nucleus.[10] ZO-2 may reduce cell proliferation by binding to and reducing the activity of the transcription complex AP1, possibly by mediating its nuclear export.[15] In addition, ZO-2 overexpression was found to down-regulate CycD1 transcription,[16] decrease its translation,

*Correspondence to: Udo Hasler; Email: Udo.Hasler@unige.ch
Submitted: 04/30/2014; Revised: 07/16/2014; Accepted: 07/16/2014
http://dx.doi.org/10.4161/15384101.2014.949091

increase its protein degradation and block cell cycle progression at the G_1/S boundary.[17] ZO-3 was proposed to be expressed more specifically in epithelia than ZO-1 and ZO-2.[18] Unlike ZO-2, ZO-3 nuclear expression has not been observed. ZO-3 depletion was found to increase CycD1 proteolysis and G_0/G_1 cell cycle retention.[19] However, the lack of an obvious phenotype of ZO-3 deficient mouse embryos [20,21] may suggest that ZO-3 can be substituted by another ZO protein.

Reabsorption of water and solutes across tubular epithelia is a fundamental function of the adult kidney. Paracellular reabsorption varies between tubular segments, is highest in the proximal tubule and gradually decreases along the tubule. Lowest levels are reached in the collecting duct (CD), a tight epithelium where the final readjustment of solute and water reabsorption occurs, critical for body homeostasis.[22,23] A hallmark of CD epithelia in healthy, adult mammalian kidney is the low rate of cell proliferation, reflecting the importance of sustained intercellular adhesion for tubular barrier function. While ZO-3 expression in the kidney CD has yet to be investigated in detail, ZO-1 and ZO-2 expression levels have been shown to be especially high at cell boundaries of this tubular segment, as compared to other tubular segments.[24,25] The roles of ZO proteins in the kidney CD are not well understood. It is feasible that ZOs may help maintain low CD paracellular permeability, not only as part of the paracellular diffusion barrier but also by restricting tubular cell proliferation.

In the present study, we examined the influence of each ZO protein on the proliferation capacity of kidney CD principal cells. We show that in addition to ZO-1 and ZO-2, ZO-3 protein is also expressed at intercellular junctions of the CD and that its expression is particularly strong in tight epithelia as compared to other tubular segments. Analysis of the effects of depleted ZO expression in $mCCD_{cl1}$ cells, a spontaneously immortalized cell line that displays highly differentiated properties of CD principal cells,[26,27] revealed that each individual ZO protein differently affects their proliferation and adhesion properties. Unexpectedly, cell cycle progression was reduced in the absence of either ZO-1 or ZO-2. ZO-3 protein abundance was found to rely on the presence of ZO-1 and its depletion had no effect on cell cycle progression but impaired cell adhesion. These observations reveal diverging, but interconnected, roles for each ZO protein on kidney CD principal cell proliferation and adhesion.

Results

ZO expression in the adult kidney

We examined ZO expression along the kidney nephron and CD. We proceeded by comparing ZO-1, -2 and -3 expression levels in the kidney of adult rats by Q-PCR analysis of isolated tubules and by immunostaining of kidney sections (**Fig. 1**). Q-PCR analysis revealed that mRNA expression levels of all 3 ZOs, and particularly ZO-3, were higher in the CD than in proximal tubules (**Fig. 1B**). No significant differences of ZO mRNA expression were observed between cortical and medullary CD. As suggested by confocal analysis, ZO total protein abundance along tubule segments was similar to that observed for ZO mRNA (**Fig. 1C**). ZO-1 expression at apical junctions was particularly strong in distal segments as compared to proximal regions. ZO-2 was also expressed at cell boundaries but was distributed in the cytoplasm to a higher extent than ZO-1. A signal corresponding to ZO-3 expression was strongest in apical junctions of tight epithelia, i.e., thick ascending limb (TAL), distal nephron and CD (**Fig. 1C** and Supplemental **Fig. 1**). Both immunofluorescence (**Fig. 1D**) and Western blot (**Fig. 1E**) revealed good expression of all 3 ZO proteins in dense $mCCD_{cl1}$ cells, a spontaneously immortalized CD principal cell line. Together, these data indicate that ZO proteins are differently expressed along the kidney tubule but that all 3 ZOs are strongly expressed both in the CD of adult animals and in $mCCD_{cl1}$ cells.

ZO expression in proliferating and non-proliferating $mCCD_{cl}$ cells

In order to validate $mCCD_{cl1}$ cells as a cell proliferation model, we examined various proliferation parameters (**Fig. 2**). After seeding, described in Materials and Methods, cell number and size increased and decreased, respectively, over time (**Fig. 2A**). Cell cycle progression decreased over time and reached a growth arrest state after 7 d of culturing (D7), as indicated by the gradual increase of G_0/G_1 phase and decrease of S phase (**Fig. 2B**). Whole-cell abundance (**Fig. 2C**) and nuclear localization (**Fig. 2D**) of CycD1, a regulator of G_0/G_1 to S phase transition, and PCNA, a key proliferation marker, decreased with cell density. Together, these observations indicate that $mCCD_{cl1}$ proliferation is sensitive to cell contact inhibition and establishes $mCCD_{cl1}$ cells as a relevant model of cell proliferation.

We compared the cellular abundance and subcellular localization of ZO proteins in proliferating and growth arrested $mCCD_{cl1}$ cells. As revealed by Western blot, ZO-1 and ZO-2 protein abundance slightly increased over time (**Fig. 3A**). ZO-3 protein abundance, however, strongly increased over time (**Fig. 3A**). Immunofluorescence revealed a signal against ZO-1 and, to a lesser extent, ZO-2 but not ZO-3 at junctional sites of low-density cells (**Fig. 3B**). All 3 ZO proteins were well expressed at intercellular junctions of high-density cells (**Fig. 3B**). Reduced expression by siRNA specifically targeting individual ZOs (siZO-1, siZO-2 and siZO-3) confirmed signal specificity (**Fig. 4C**). The transcription factor ZONAB was previously shown to regulate cell cycle proliferation and differentiation in a cell density-dependent manner under the control of ZO-1.[11,12,28] We examined ZONAB expression and subcellular localization in $mCCD_{cl1}$ cells. Two ZONAB isoforms (ZONAB-long and ZONAB-short) were previously reported in MDCK cells.[14] These differ in size by alternative splicing but both associate with intercellular junctions.[14] Western blot revealed that both ZONAB isoforms were expressed in $mCCD_{cl1}$ cells and their protein abundance decreased with cell density (**Fig. 3A**). As revealed by immunofluorescence, ZONAB was expressed in the nucleus and cytoplasmic compartments of sparse cells (**Fig. 3B**). These expression levels decreased as cell density increased (**Fig. 3B**). Signal specificity was verified by siRNA-mediated depletion of ZONAB expression (**Fig. S2**). Surprisingly, a signal at intercellular junctions was also observed but only in sparse,

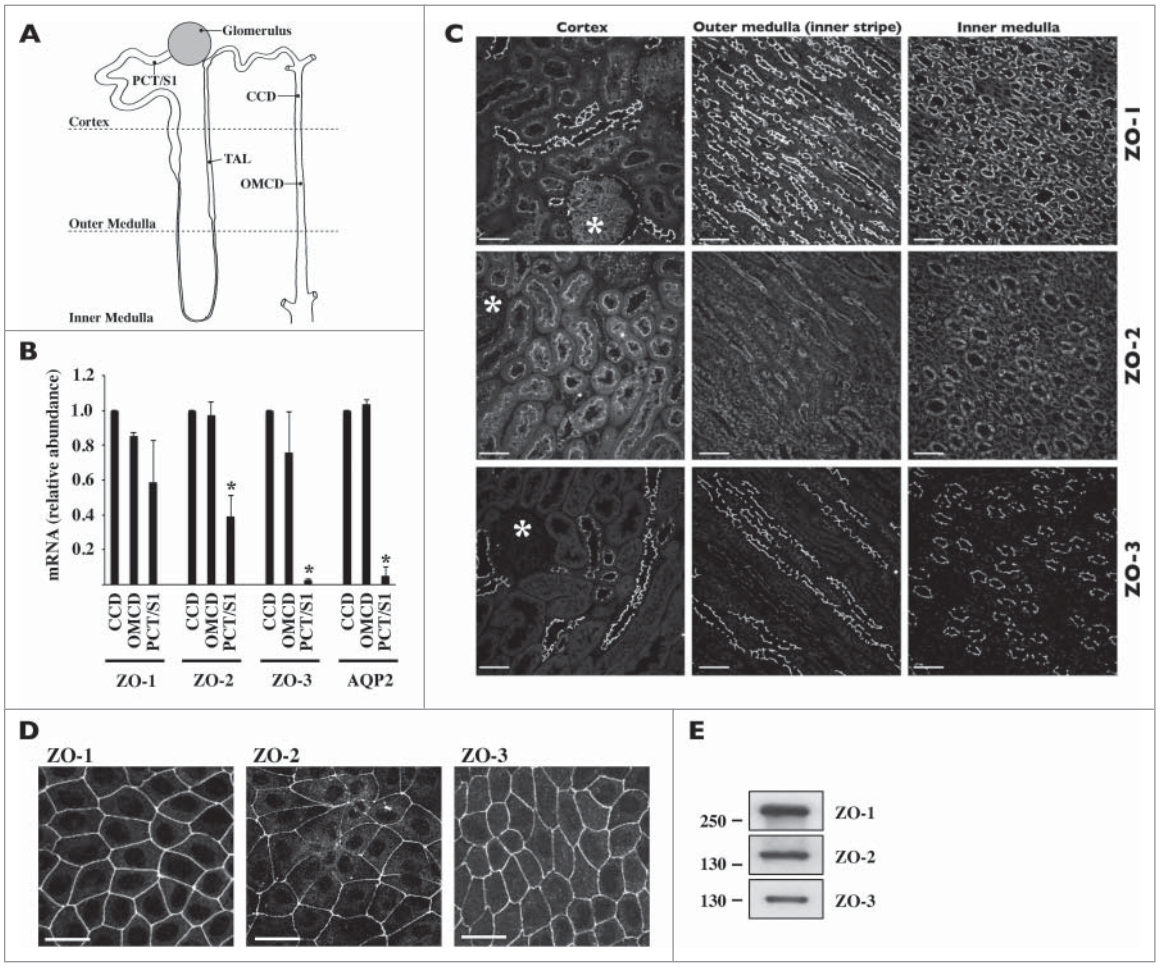

Figure 1. Expression of ZO proteins along the kidney tubule. (**A**) Cartoon depicting the glomerulus and various regions of the nephron and collecting duct. PCT/S1, S1 segment of the proximal tubule; TAL, thick ascending limb of Henle's loop, CCD, cortical collecting duct; OMCD, outer medullary collecting duct. (**B**) mRNA expression levels of ZO-1, ZO-2, ZO-3 and AQP2, used as a collecting duct-specific marker, were compared by Real-Time PCR between segments of isolated kidney tubules. Data is represented as fold difference of mRNA expression over values obtained in cortical collecting duct and is expressed as the mean ± SEM of data from 3 animals. (**C**) and (**D**) Confocal z-stacks of ZO-1, ZO-2 and ZO-3 immunostaining of the cortex, outer medulla and inner medulla of kidney slices (**C**) and dense $mCCD_{cl1}$ cells (**D**). Images are representative of those acquired from 3 animals and at least 3 *in vitro* experiments. Bar, 10 μm. Glomeruli are indicated by an asterisk. (**E**) Western blot of whole-cell ZO-1, ZO-2 and ZO-3 protein depicting their expression in dense $mCCD_{cl1}$ cells.

not dense, cells (**Fig. 3B**). However, this could be non-specific since signal strength was not reduced by ZONAB silencing (**Fig. S2**). Alternatively, it might represent a ZONAB isoform stably expressed at intercellular junctions.

ZO-1 and ZO-2 were shown to be present in the nucleus of tubular cells.[10,24] All 3 ZO proteins contain nuclear localization and nuclear export signals,[28,29] suggesting that all 3 ZOs could theoretically localize to the nucleus. Peripheral and cytosolic staining was bright and could potentially mask nuclear staining. This led us to examine nuclear ZO expression by an alternative method, i.e., Western blotting of cytosolic and nuclear extracts, as previously performed in our laboratory on $mCCD_{cl1}$ cells.[30] All 3 ZO proteins were found to be present in the nucleus of $mCCD_{cl1}$ cells (**Fig. S3**). ZO-1 and ZO-2 nuclear expression slightly increased with cell density. Unexpectedly, while ZO-3 cytosolic expression slightly increased with cell density, its nuclear expression increased dramatically. Reduced ZO-3 cytosolic and nuclear expression by siZO-3 confirmed signal specificity (**Fig. 6B**). As expected, and corroborating our confocal microscopy analysis (**Figs. 2D** and **3B**), ZONAB, CycD1 and PCNA cytosolic and nuclear expression decreased with cell density (**Fig. S3**).

To study ZO protein expression in newly proliferating cells, we performed a scratch assay on high-density cells, which form a quiescent monolayer (**Figs. 3C** and **3D**). Although typically used for analysis of cell migration properties, this assay is well suited as a model of cell proliferation since both processes are closely linked. As expected, cell proliferation was significantly increased in regions bordering the scratch wound as compared to more distant regions, as indicated by high levels of nuclear CycD1 and

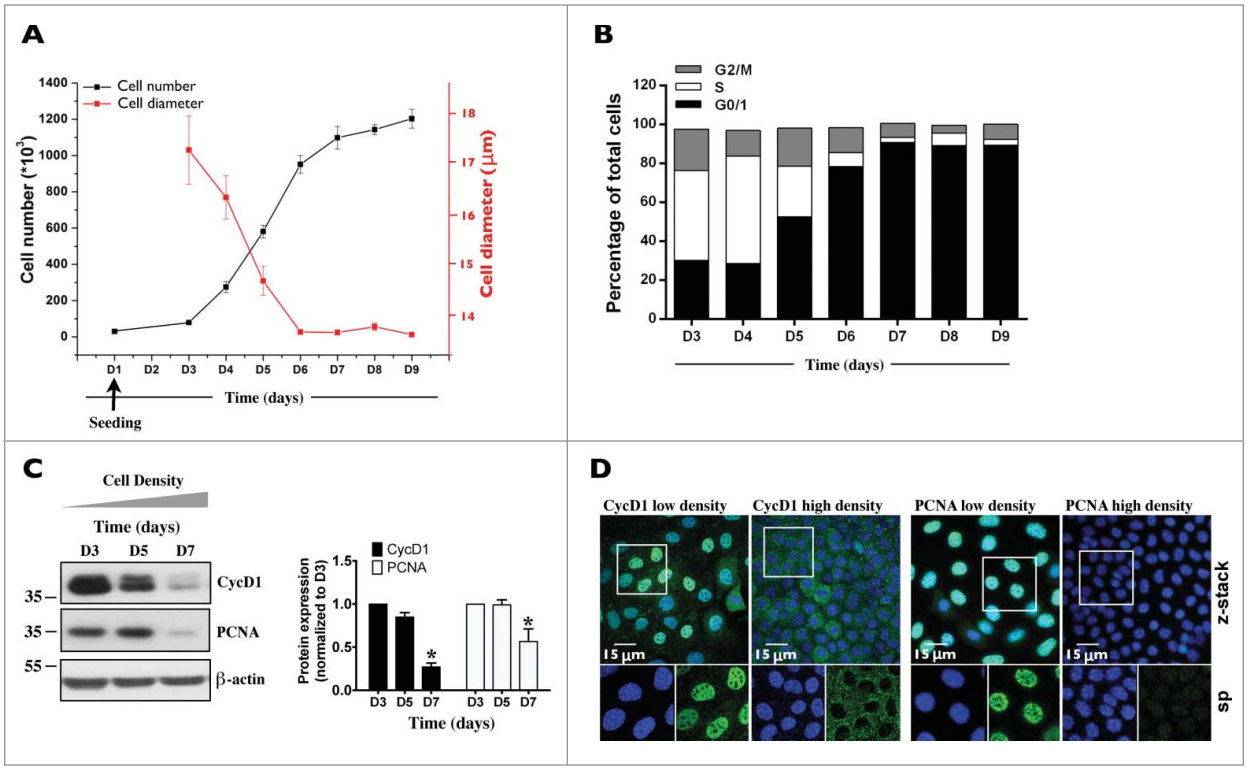

Figure 2. Characterization of $mCCD_{cl1}$ cell proliferation. Cells were seeded at day 1 (D1) as described in Materials and Methods and various parameters of cell proliferation were examined over time (D1 - D9). (**A**) Cell number was estimated by trypsinizing and counting cells with a hemocytometer. Cell diameter was estimated by ImageJ analysis of images taken prior to cell trypsinization. Data is represented as fold increase of cell number (black squares) and cell area (red squares) over values obtained 3 d (D3, for cell number analysis) and 6 d (D6, for cell area analysis) after seeding. (**B**) Cell cycle analysis by flow cytometry. Data shown is representative of one of 3 similar experiments. (**C**) Western blot of whole-cell CycD1 and PCNA. β-actin was used as a loading control. Quantification of data, shown at right, is represented as fold difference of protein expression over values obtained at D3 and is expressed as the mean ± SEM of 3 independent experiments. (**D**) Confocal z-stacks of CycD1 (green, left panels) and PCNA (green, right panels) depicting their nuclear expression in low (D3) and high (D7) density cells. Enlarged single-plane (sp) images of Hoechst (blue) or immunofluorescence staining of cells outlined by a white rectangle are also shown below. One of 3 similar experiments is shown. Bar, 15 μm.

PCNA (**Fig. 3C**). Reflecting observations made between low- and high-density cells (**Fig. 3B**), ZONAB expression was especially high along the scratch wound while ZO-1 and ZO-2 expression at intercellular junctions was slightly lower in cells bordering the scratch wound than in more distant regions (**Fig. 3D**). Remarkably, ZO-3 expression was dramatically reduced in regions bordering the scratch wound, to a greater extent than that observed for ZO-1 and ZO-2 (**Fig. 3D**).

Together, these observations reveal that ZO protein expression at intercellular junctions increases as contacts between neighboring cells are progressively established, and that ZO-3 expression dramatically increases with cell density. Differences of abundance and subcellular localization between ZO proteins in proliferating and growth arrested cells indicate that each ZO protein may play specific roles in $mCCD_{cl1}$ proliferation.

ZO proteins differentially influence $mCCD_{cl1}$ cell proliferation and adhesion

To test whether ZO proteins affect $mCCD_{cl1}$ proliferation, cells were transfected with siRNA targeting each individual ZO and various experiments were performed on cells 1–6 d post-transfection (referred to as T1-T6 throughout the manuscript). Reflecting changes of ZO protein expression (**Fig. 3A**), ZO-3 mRNA, but not ZO-1 and -2 mRNA, increased with cell density (**Fig. 4A**). siRNA against individual ZOs reduced the expression levels of targeted ZO mRNA from T1 to T4 without significantly affecting mRNA levels of non-targeted ZOs (**Fig. 4A**), validating siRNA silencing efficiency and specificity. Each siRNA species effectively reduced target gene protein expression as well (**Figs. 4B** and **4C**). siRNA targeting individual ZOs had no obvious effect on the distribution of non-targeted ZOs at intercellular junctions (**Fig. 4C**). However, both Western blot and confocal microscopy analysis revealed that siZO-1 dramatically reduced ZO-3 protein abundance (**Figs. 4B** and **4C**). On the other hand, although variable results were obtained at T2, siZO-3 had no significant global effect on ZO-1 protein abundance (**Fig. 4B**). Another unrelated siZO-1 species (**Table 1**) similarly reduced ZO-3 protein, but not mRNA expression (not shown). Low levels of ZO-3 protein expression by siZO-1 abided even in the presence of inhibitors of lysosomal or proteasomal protein degradation (**Fig. S4**), suggesting that ZO-3 mRNA translation might be attenuated in the absence of ZO-1.

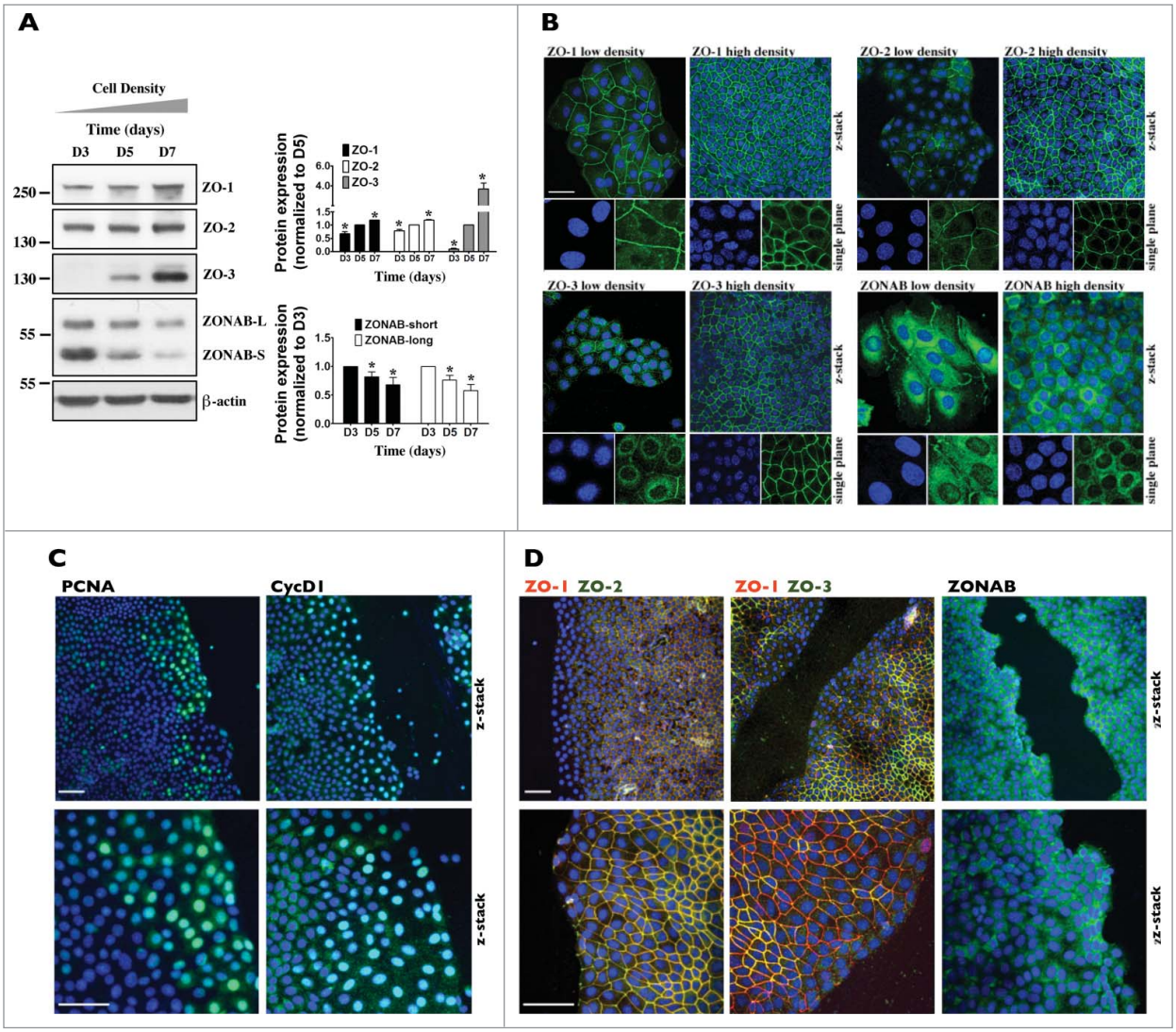

Figure 3. ZO-3 abundance and expression at junctions is dramatically increased in confluent $mCCD_{cl1}$ cells. (**A**) Western blot of ZO-1, ZO-2, ZO-3 and ZONAB 3, 5 and 7 d (D3, D5 and D7) after seeding. β-actin was used as a loading control. Quantification of data, shown at right, is represented as fold difference of protein expression over values obtained at D5 (for ZO proteins) and D3 (for ZONAB) and is expressed as the mean ± SEM of 3 independent experiments. (**B**) Immunofluorescence of low- and high-density cells. Shown are confocal z-stacks of ZO-1, ZO-2, ZO-3 and ZONAB (all green) depicting their expression at junctional sites (and nuclear expression for ZONAB) in low (D3) and high (D7) density cells. Enlarged single-plane images of Hoechst (blue) or immunofluorescence staining of cells are also shown below. Bar, 10 μm. (**C** and **D**) Immunofluorescence of high-density cells 6 h after scratch. Shown are confocal z-stacks of PCNA (green) and CycD1 (green) (C), ZONAB (green) (**D**) and double-stained confocal z-stacks of ZO-1 (red) / ZO-2 (green) and ZO-1 (red) / ZO-3 (green) (**D**), depicting their expression at junctional sites (and nuclear expression for PCNA, CycD1 and ZONAB) of cells bordering scratch wounds and of cells located at more distant regions. Enlarged images of Hoechst (blue) or immunofluorescence staining of cells bordering scratch wounds are also shown below. Bar, 30 μm. For (**B–D**), one of 3 similar experiments is shown.

We examined whether ZO protein silencing affects cell number from T1 - T4. Silencing of ZO-1 and ZO-3 reduced cell number as compared to the control group (**Fig. 5A**). Although not significantly different, there was a tendency of ZO-2 silencing to reduce cell number as well. Reduced cell number persisted after longer periods of time (e.g. siZO/control cell number ratios at T6 were: scramble siRNA: 1 ± 0.08; siZO-1: 0.66 ± 0.05; siZO-2: 0.83 ± 0.04; siZO-3: 0.74 ± 0.07) and was accompanied by altered cell confluence and size. While near complete confluency was reached at T4 in both control cells and cells transfected with any siZO, at earlier times cell confluence was slightly (but not significantly) decreased by siZO-1 and siZO-2 and was significantly decreased by siZO-3 (**Fig. 5B**). Reflecting changes of cell number and confluency, the size of control cells gradually decreased over time as cell confluence increased (**Fig. 5C**). On the other hand, while not apparent at T1, cell size was increased by silencing of any ZO protein and remained elevated even when near complete confluency was reached at T4, particularly in cells transfected with siZO-1 or siZO-2 (**Fig. 5C**). Neither cell necrosis nor apoptosis was increased by any siZO

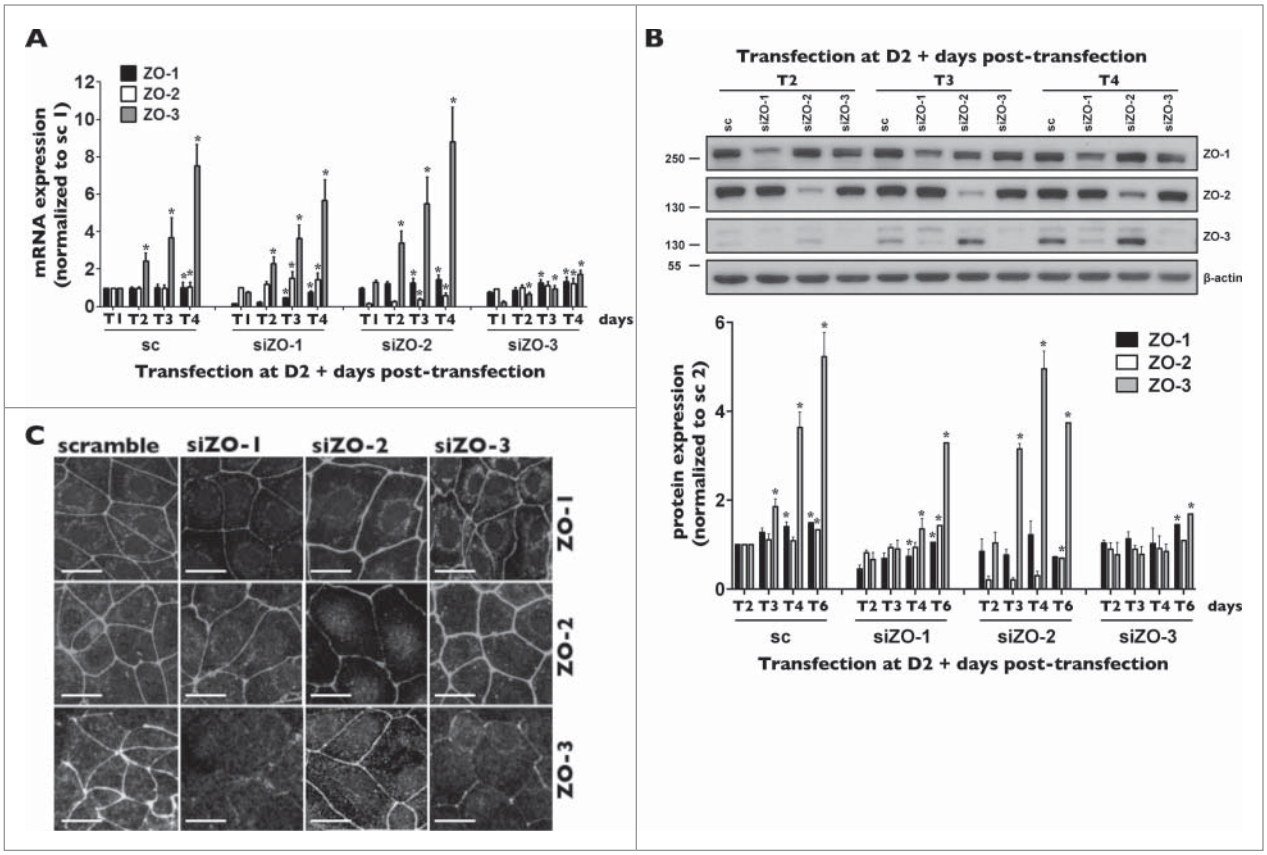

Figure 4. ZO-3 protein expression relies on the presence of ZO-1 in $mCCD_{cl1}$ cells. (**A** and **B**) Cells were transfected 1 day after seeding with siRNA (sc) or siRNA against ZO-1 (siZO-1), ZO-2 (siZO-2) or ZO-3 (siZO-3) and mRNA (**A**) and protein (**B**) were isolated 1 - 6 d post-transfection (T1 - T6). Data is represented as fold difference of mRNA expression over values obtained in cells transfected with scrambled siRNA at T1 (for mRNA analysis) or at T2 (for protein analysis) and is expressed as the mean ± SEM of 4 independent experiments. Significant change of expression ($P \leq 0.05$) within a same experimental group is depicted by an asterisk. (**C**) Confocal z-stacks of ZO-1, ZO-2 and ZO-3 depicting their expression in cells transfected with either scrambled siRNA, siZO-1, siZO-2 or siZO-3 at T3. One of 3 similar experiments is shown. Bar, 10 μm.

(**Fig. 5D**), indicating that decreased cell number by siZOs does not arise from an increase of cell death.

We next examined whether ZO protein silencing affects cell cycle progression. G_0/G_1 and S phases of control cells steadily increased and decreased, respectively, from T1 to T6 (Supplemental **Fig. 5**). As compared to control cells, siZO-1 or siZO-2 transfection increased the G_0/G_1 phase and decreased the S phase at T1 and T2, i.e., at which time similar cell number and confluency between experimental groups was observed (**Fig. 5E**, left panel). This indicates that cell cycle progression was delayed at the G_0/G_1 phase. At higher confluency (T3 -T6), cell proliferation abated in control cells and cell cycle progression reached low levels observed in cells transfected with siZO-1 or siZO-2 (Supplemental **Fig. 5**). Contrary to the effects of ZO-1 and ZO-2 silencing, cell cycle progression was not significantly altered by siZO-3 transfection. We additionally examined whether ZO silencing affects cell cycle progression during early stages of cell growth (**Fig. 5E**, right panel). For this, we transfected cells with siRNA, re-seeded cells 24 h post-transfection and measured the cell cycle 24 h later. While siZO-1 similarly affected cell cycle progression of sparse cells and T1 and T2 cells, siZO-2 only modestly reduced cell cycle progression of sparse cells. Possibly, unlike siZO-1, decreased cell cycle progression by siZO-2 may only arise once cell-cell contacts are established. This suggests that ZO-1 and ZO-2 each regulate cell cycle progression via different mechanisms.

Interestingly, silencing of ZO-3, and to a lesser extent ZO-1, but not ZO-2, unexpectedly increased cell detachment (**Figs. 5F** and **5G**). Phrase-contrast microscopy revealed that cell detachment already occurred at T1, persisted well after full confluence was reached (T6) and also occurred in sparse siZO-3-transfected cells (T1 cells that were re-seeded and analyzed 1 day later). Cells transfected with either siZO-1 or siZO-3 grown to high-density (T6) also lacked domes (**Fig. 5G**). These correspond to tight monolayers lifted from the plastic support as a consequence of vectorialized ion transport.[31,32] The absence of these structures lends additional evidence of deficient cell adhesion.

Together, these observations suggest that silencing of either ZO-1 or ZO-2 decreases $mCCD_{cl1}$ cell cycle progression while ZO-3 deficiency decreases cell adhesion.

Table 1. RT-PCR primer sequences and siRNA sequences

Real-Time PCR primer sequences (mouse unless specified)		
Targeted gene	**Forward**	**Reverse**
P_0	AATCTCCAGAGGCACCATTG	GTTCAGCATGTTCAGCAGTG
P_0 (rat)	CCTTCTCCTTCGGGCTGATC	GGGCTGTAGATGCTGCCATT
ZO-1	GCCGCTAAGAGCACAGCAA	TCCCCACTCTGAAAATGAGGA
ZO-1 (rat)	CTG AAG AGG ATG AAG AGT ATT ACC	TGA GAA TGG ACT GGC TTG G
ZO-2	GTTTGCCGTTCAGCAGCTTAG	CTTCAAAACCTCGGTCGTCAT
ZO-2 (rat)	TAA AGG TGA AAC CGT GAC CA	CAC AGG CCA GGA TGT CTC TA
ZO-3	TGCACCAAAACAGCCAACG	CTCACCCCATGATCGACCT
ZO-3 (rat)	GTG AAA CGA AGA AAC AGC GA	TGG ACA CTC CGT TGA TCT GT
ZONAB	AATGGTTCAACGTCAGAAATGGA	CGCAGATACTTGCGTGGGTT
CyclinD1	CTCCGTATCTTACTTCAAGTGCG	CTTCTCGGCAGTCAAGGGAA
p21	GCAGATCCACAGCGATATCCA	GGTCGGACATCACCAGGATT
Claudin-4	AAGTGCACCAACTGCATG GA	GGCTCCGGCGGTGATC
Claudin-8	GCAACCTACGCTCTTCAAATGG	TTCCCAGCGGTTCTCAAACAC
Occludin	GCCCCGGAAGATCGTGTTT	TAGTCAGGTACTGGGTTGAGG
	siRNA sequences	
scramble	5′- GCCACUCGUUUGUCGCCCUUGUAAA-3′	
ZO-1_1	5′- GGUCUUCGAUUGGCCAGCCAUAUAU-3′	
ZO-1_2	5′- GCAAAGAGAUGAGCGGGCUACCUUA-3′	
ZO-2	5′- CGUGACCCUGCAGAAGGAUUCCAAA-3′	
ZO-3	5′- CCAGAUCCUUAAGACCUGCACCAAA-3′	
ZONAB	5′- UAUAGUUGUAGGGACGUCGGAAUCC-3′	
CyclinD1	5′- ACUUGAAGUAAGAUACGGAGGGCGC-3′	
Occludin	5′-GGAGGAAGCCUAAACUACCCUUAUA-3′	
β1-integrin	5′-CAGAGGCUCUCAAACUAUAAAGAAA-3′	
p21	5′-AUAGAAAUCUGUCAGGCUGGUCUGC-3′	

Roles of ZONAB, CycD1 and p21 in decreased $mCCD_{cl1}$ proliferation by ZO-1 and ZO-2 silencing

Since ZO-1 or ZO-2 silencing blocked the cell cycle progression at G_1/S phase, we examined the roles of ZONAB, CycD1 and the cell cycle inhibitor p21, all of which regulate G_1/S transition, in reduced $mCCD_{cl1}$ cell proliferation. Each gene was differently affected by ZO-1 or ZO-2 silencing. Overall, ZONAB mRNA was not significantly affected by ZO protein silencing (Supplemental **Fig. 6**). While ZONAB protein expression was not affected by siZO-2 (**Fig. 6A**), siZO-1 decreased whole-cell and nuclear ZONAB-long but not ZONAB-short expression (**Figs. 6A** and **6B**). Cytosolic ZONAB-long abundance, on the other hand, was not decreased by siZO-1 (**Fig. 6B**). Contrary to ZONAB, CycD1 mRNA and protein were increased by siZO-1 while siZO-2 decreased CycD1 protein but not mRNA expression (**Figs. 6A, 6B** and Supplemental **Fig. 6**). Finally, p21 protein abundance was increased by siZO-1 and, to a lesser extent, by siZO-2 (**Figs. 6A** and **6B**). Interestingly, increased whole cell and nuclear expression of CycD1 and p21 by siZO-1 were also observed in cells transfected with siZO-3 (**Figs. 6A** and **6B**), which does not significantly affect cell cycle progression (**Fig. 5E**). Similar to siZO-1, siZO-3 decreased whole cell and nuclear ZONAB-long expression, but, unlike siZO-1, also decreased ZONAB-short expression.

S phase progression requires nuclear CycD1 export and proteolytic degradation,[33,34] indicating that high levels of nuclear CycD1 may interfere with S phase progression in ZO-1-deficient cells. This led us to examine its role and that of p21 in decreased cell cycle progression by siZO-1. Cell cycle progression was decreased by CycD1 silencing but was not altered by p21 silencing (**Fig. 6C**). Interestingly, ZO-1/CycD1 co-silencing further decreased cell cycle progression while the effects of siZO-1 were completely abolished by simultaneous p21 silencing. Since ZONAB-long expression is decreased by siZO-1, we also examined the effects of ZONAB depletion by siRNA on cell cycle progression. As expected, siRNA against ZONAB (siZONAB) decreased cell cycle progression (**Fig. 6D**). Unexpectedly, but similar to the effect of siZO-1, siZONAB increased both CycD1 and p21 protein abundance (**Fig. 6E**).

Together, these observations indicate that decreased cell cycle progression by ZO-2 silencing arises at least in part from decreased CycD1 expression. Decreased cell cycle progression by siZO-1, on the other hand, is associated with decreased nuclear ZONAB-long that in turn may increase p21 nuclear expression. Cell cycle progression in siZO-1-transfected cells is completely restored by p21 silencing, pointing to a key role for p21 in decreased cell cycle progression by siZO-1.

Decreased cell adhesion by ZO-3 silencing relies on a multifactorial process

In addition to its key role in regulating cell proliferation, CycD1 was also shown to negatively influence cell adhesion.[35–37] Since CycD1 and p21 abundance are increased by siZO-3 (**Figs. 6A** and **6B**) we examined whether silencing of CycD1 can alter the effects of siZO-3. Since p21 is a negative regulator of

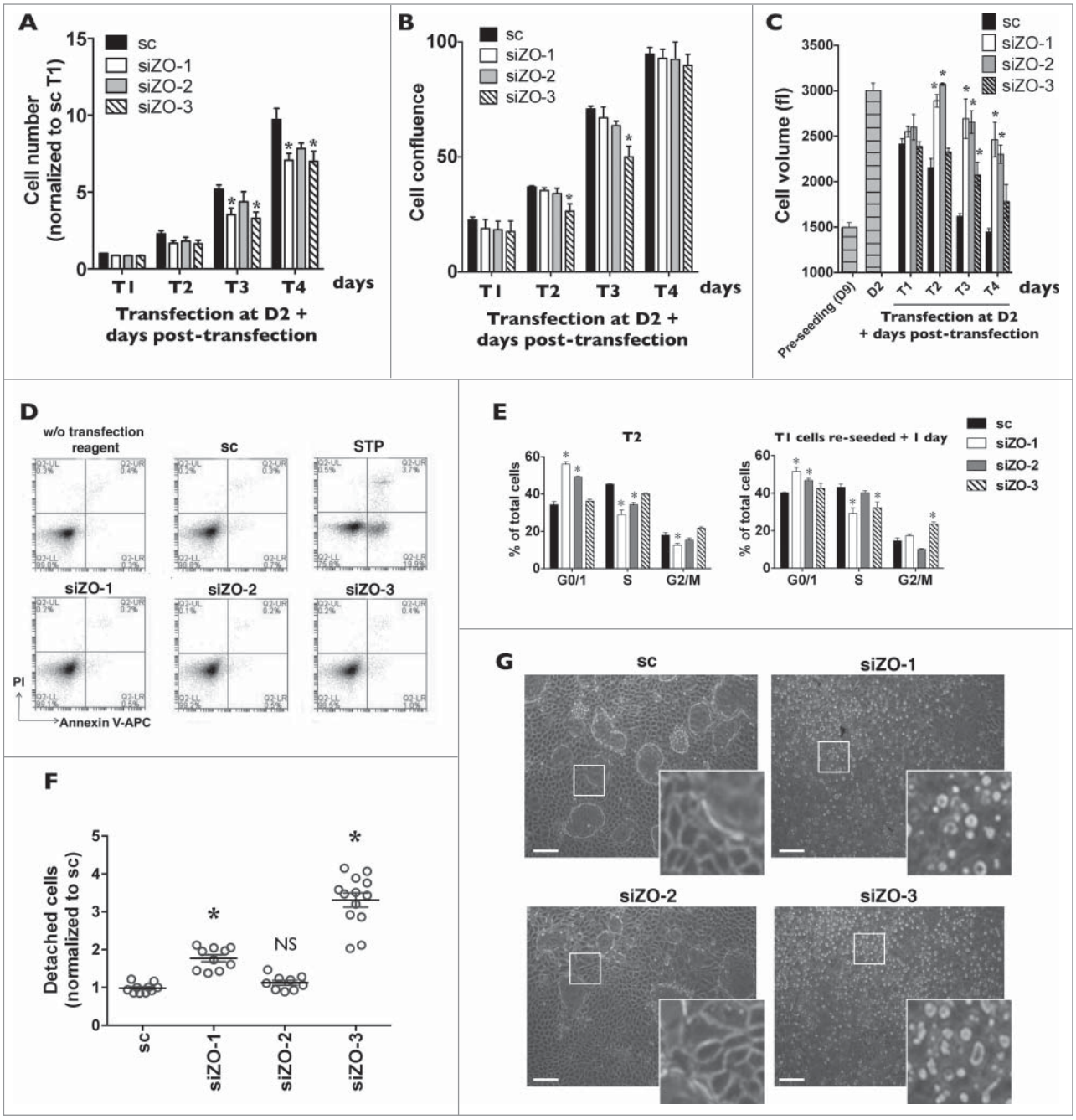

Figure 5. Decreased expression of each ZO protein differently affects $mCCD_{cl1}$ cell cycle progression and adhesion. (**A-C**) Cells were transfected 1 day after seeding with scrambled siRNA (sc) or siRNA against ZO-1 (siZO-1), ZO-2 (siZO-2) or ZO-3 (siZO-3) and cell number (**A**), cell confluence (**B**) and cell volume (**C**) were measured 1–4 d post-transfection (T1 - T4). Data is expressed as the mean ± SEM of 4 independent experiments. Cell number is represented as fold difference of siZO data over values obtained in cells transfected with scrambled siRNA at T1. (**D**) Cell death analysis by flow cytometry of cells transfected with scrambled siRNA or siRNA against ZOs at T3. Staurosporine (STP, 500 nM for 24 h) was used as a positive control for cell apoptosis. (**E**) Cell cycle analysis by flow cytometry of cells transfected with scrambled siRNA or siRNA against ZOs at T2 (left panel) or of cells exposed to siRNA for 1 day (T1), re-seeded and analyzed 1 day later (right panel). Data is expressed as the mean percentage of G_0/G_1, S and G_2/M phase cells ± SEM of 4 independent experiments. (**F**) Quantification of cell detachment by flow cytometry of cells transfected with scrambled siRNA or siRNA against ZOs. Data is represented as fold difference of detached cells over values obtained in cells transfected with scrambled siRNA at T2 and is expressed as the mean ± SEM of 5 independent experiments performed in duplicate. NS: no significant difference. (**G**) Phase-contrast microscopy of high-density cells (T6) illustrating the absence of domes and increased number of detached cells in cells transfected with siZO-1 and siZO-3 as compared to cells transfected with scrambled siRNA or siZO-2. Enlarged images of cells outlined by a white rectangle are shown in inserts. One of 4 similar experiments is shown. Bar, 50 μm.

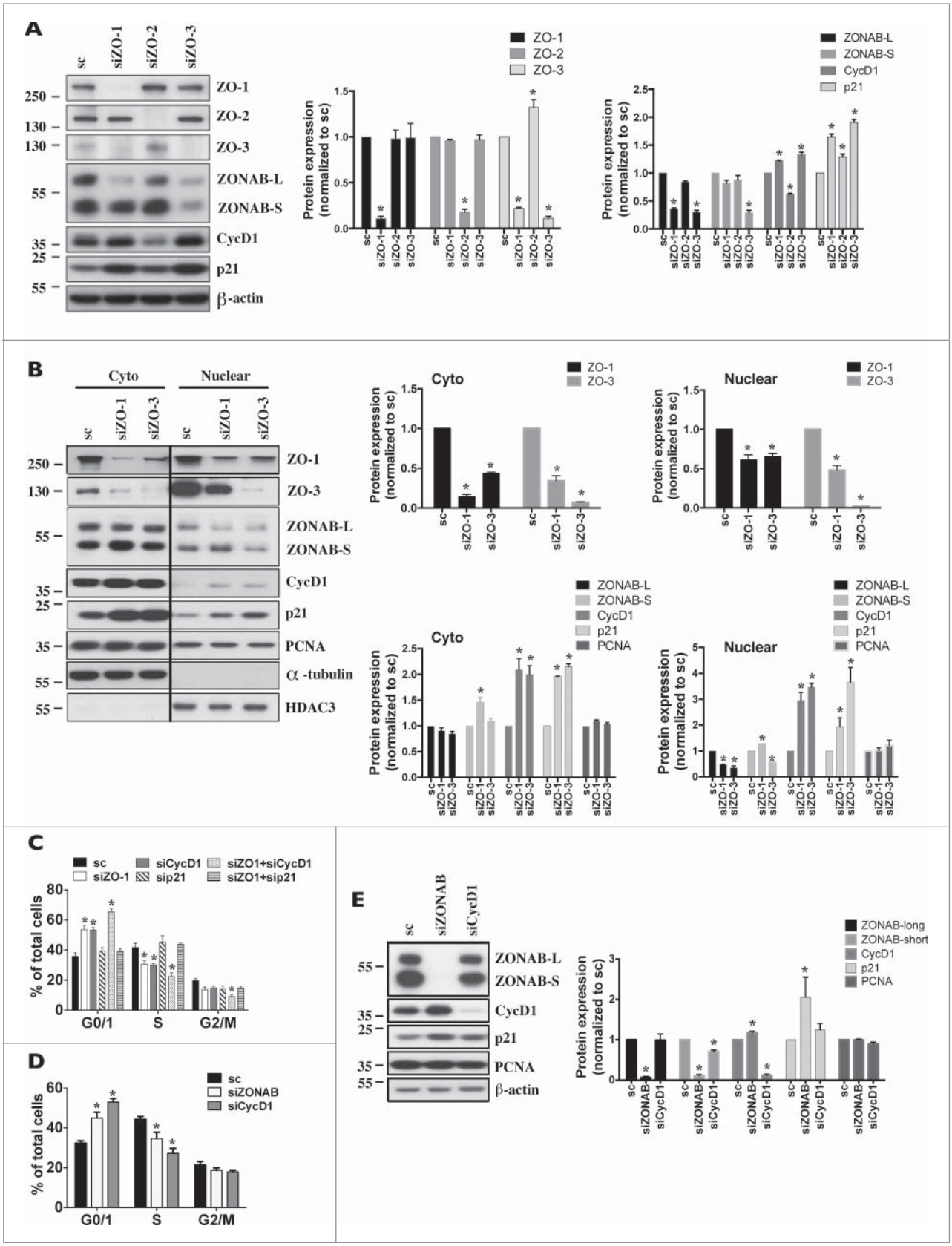

Figure 6. For figure legend, see page 3068.

CycD1, as expected, cell detachment increased in cells transfected with siRNA against p21 (sip21) and remained elevated in cells transfected with both sip21 and siZO-3 (Supplemental **Fig. 7A**). CycD1 silencing, on the other hand, significantly decreased but did not abolish cell detachment by siZO-3 (**Figs. 7A** and **7B**). This suggests that increased CycD1, but not p21, expression may participate in cell detachment by ZO-3 silencing.

We examined 2 other factors that may be involved in decreased cell adhesion by siZO-3, namely integrins and occludin. ZO-1 was previously shown to form a complex with $\alpha_5\beta_1$-integrin and regulate lamellae formation in epithelial cells.[38,39] As expected, siRNA against β_1-integrin, the most prevalent integrin protein,[40] promoted cell detachment (**Fig. 7C**). While ZO-3 silencing did not alter total protein abundance of β_1-integrin (**Fig. 7D**), it did affect its intracellular distribution. This was illustrated by immunostaining analysis of the active form of β_1-integrin using a β_1-integrin active epitope antibody (**Fig. 7E**). Visibility of active β_1-integrin is high in lamellipodium and focal adhesions of sparse cells and gradually decreases with cell confluency. This may at least partly result from a switch of active β_1-integrin by another integrin protein. Although prominent in about 30% of control cells, active β_1-integrin was virtually absent in cells transfected with siZO-3. This illustrates the principle that ZO-3 silencing may alter integrin subcellular distribution and consequently cell adhesion efficiency.

Occludin is well expressed in kidney CD,[24] interacts with ZOs [41,42] and may increase cell adhesiveness.[43–46] We noticed a remarkable correlation between ZO-3 and occludin expression in proliferating $mCCD_{cl1}$ cells. Similar to ZO-3, whole-cell occludin protein abundance was low in sparse cells and increased with cell density (**Fig. 7F**). Its expression at intercellular junctions also increased with cell density and scratch wound assay revealed strongly decreased expression of both occludin and ZO-3 at intercellular junctions of cells bordering scratch wounds (**Fig. 7G**). On the other hand, claudin-4 and claudin-8, 2 major claudins of the kidney CD,[23] appeared at intercellular junctions well before ZO-3 and occludin (**Figs. S7B** and **C**). As revealed by Western blot and immunostaining, siZO-3, but not siZO-1 or siZO-2, dramatically reduced occludin abundance but not claudin-4 or claudin-8 abundance (**Fig. 7B; Figs. S7D** and **E**). Moreover, cell detachment was significantly increased by siOccludin (**Fig. 7C**). These observations indicate that decreased occludin expression could contribute to increased cell detachment by siZO-3.

Together, these data suggest that a cohort of factors mediates increased cell detachment by ZO-3 silencing. These include increased CycD1 expression, altered subcellular integrin distribution and decreased occludin expression at intercellular junctions.

Discussion

The most apical component of the intercellular junctional complex consists of TJs that play key roles in epithelial tissue function. TJs are foremost recognized as paracellular diffusion barriers. In the kidney, paracellular permeability is thought to be principally determined by charge selectivity by claudins that are differently expressed in each tubule segment.[23] More recently, TJs were shown to recruit molecules that participate in cell polarization, differentiation and proliferation.[10] These cellular properties rely on the scaffolding function of ZO proteins that interact with both transmembrane junctional proteins and multiple signaling molecules. Because low cell proliferation likely benefits intercellular adhesion, and thus diffusion barrier efficiency, it stands to reason that ZO proteins influence CD permeability not only as part of a diffusion barrier but also by helping to maintain the intercellular seal by restricting cell proliferation. The aim of this study was to establish the influence of ZO proteins on kidney CD principal cell proliferation. We show that all 3 ZO proteins are strongly expressed in kidney CD and in dense $mCCD_{cl1}$ cells. We unexpectedly found that deficiency of either ZO-1 or ZO-2 reduced rather than increased $mCCD_{cl1}$ cell cycle progression, as might have been anticipated. We show that the effect of ZO-1 silencing relies on p21 while reduced cell cycle progression by ZO-2 silencing is associated with decreased CycD1 abundance. We also found that $mCCD_{cl1}$ adhesion critically relies on the presence of ZO-3 protein, which in turn depends on ZO-1 expression. We show that decreased cell adhesion by ZO-3 silencing partly results from increased CycD1 expression. These results reveal distinct, but interconnected roles for each ZO protein on kidney CD principal cell proliferation and adhesion that together help maintain CD epithelial properties.

Previous experimental evidence suggest that rather than forming trimeric ZO-1/ZO-2/ ZO-3 complexes, ZO proteins exist as

Figure 6 (See previous page). Decreased cell cycle progression by ZO-1 and ZO-2 silencing is respectively associated with increased p21 and decreased CycD1 expression. (**A**) Cells were transfected 1 day after seeding with scrambled siRNA or siRNA against ZO-1 (siZO-1), ZO-2 (siZO-2) or ZO-3 (siZO-3) and whole cell protein expression was analyzed by Western blot 2 d later (at T2). β-actin was used as a loading control. Quantification of data, shown at right, is represented as fold difference of protein expression over values obtained in cells transfected with scrambled siRNA and is expressed as the mean ± SEM of 3 independent experiments. (**B**) Cytosolic and nuclear extracts were prepared from cells transfected 1 day after seeding with scrambled siRNA (sc), siZO-1 or siZO-3 at T3. Protein expression in both cell fractions was analyzed by Western blot. α-tubulin was used as a loading control for cytosolic extracts and histone deacetylase 3 (HDAC3) was used as a loading control for nuclear extracts. Quantification of data, shown at right, is represented as described in (A). (**C**) Cell cycle analysis by flow cytometry at T2 of cells transfected 1 day after seeding with either scrambled siRNA (sc), siZO-1, siRNA against CycD1 (siCycD1), siRNA against p21 (sip21) or with both siZO-1/siCycD1 or siZO-1/sip21. Data is expressed as the mean percentage of G_0/G_1, S and G_2/M phase cells ±SEM of 3 independent experiments. (**D**) Cell cycle analysis by flow cytometry at T2 of cells transfected 1 day after seeding with scrambled siRNA (sc) or siRNA against ZONAB (siZONAB) or siCycD1. Data is expressed as the mean percentage of G_0/G_1, S and G_2/M phase cells ± SEM of 4 independent experiments. (**E**) Whole-cell protein lysates were prepared from cells transfected as described in (**D**). Protein expression was analyzed by Western blot. β-actin was used as a loading control. Quantification of data, shown at right, is represented as fold difference of protein expression over values obtained in cells transfected with scrambled siRNA and is expressed as the mean ± SEM of 3 independent experiments.

independent ZO-1/ ZO-2 and ZO-1/ ZO-3 complexes.[47] Intriguingly, we show that ZO-3 protein expression in $mCCD_{cl1}$ cells critically relies on the presence of ZO-1 but not ZO-2. This is in line with a recently described reduction of ZO-3 expression by simultaneous ZO-1 and ZO-2 knock-down in MDCK cells.[48,49] In those studies, ZO-1/ZO-3 dimerization was found to stabilize steady state ZO3 protein levels. In our study, ZO-1 suppression had no effect on ZO-3 mRNA but dramatically

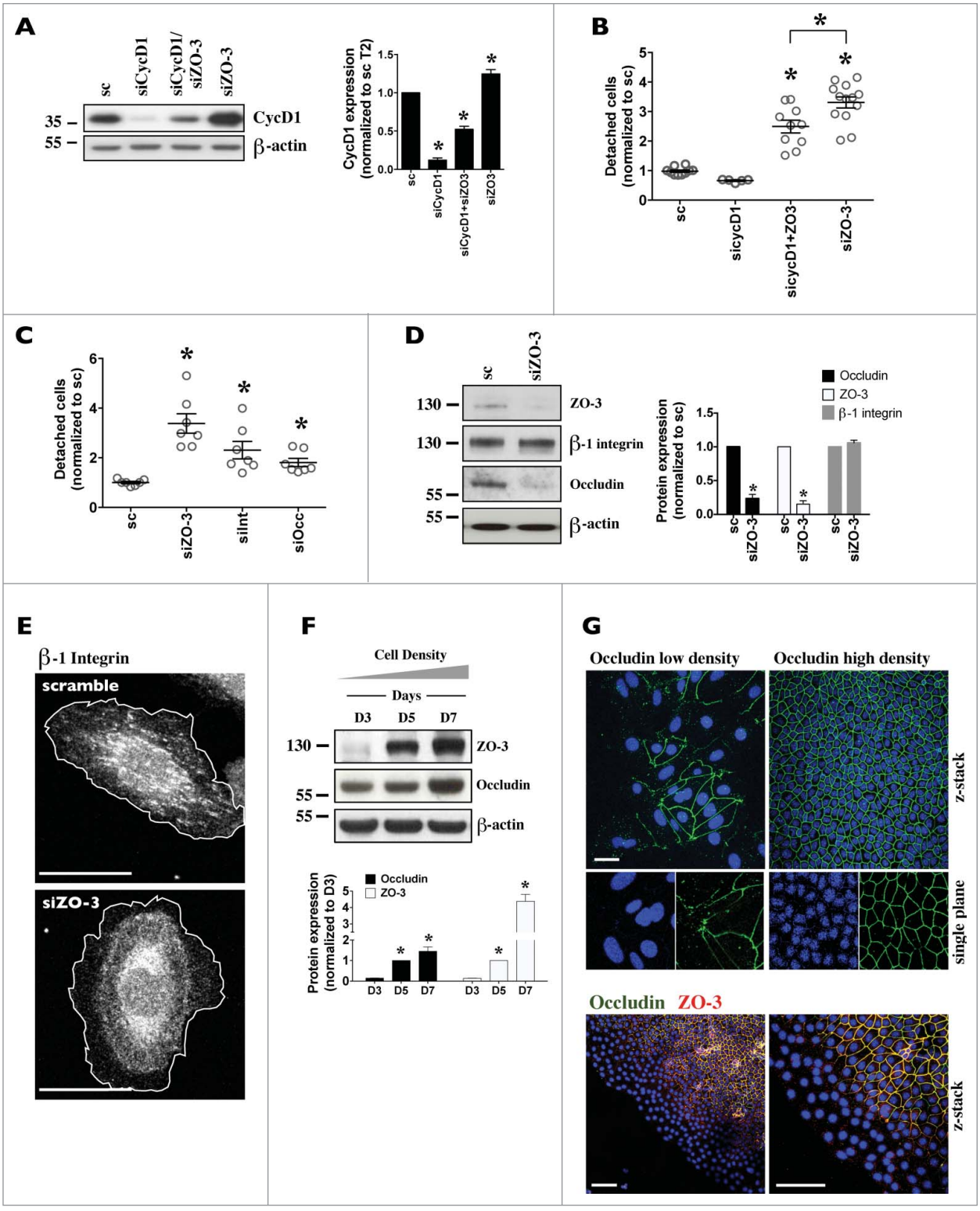

Figure 7. For figure legend, see page 3070.

decreased expression levels of ZO-3 protein. This was not prevented by inhibition of either lysosomal or proteasomal protein degradation. This points to the possibility that ZO-3 mRNA translation requires ZO-1.

We show that low levels of ZO-3 in sparse $mCCD_{cl1}$ cells dramatically increase with cell density and that ZO-3 expression in proliferating $mCCD_{cl1}$ cells is preceded by ZO-1 and ZO-2 expression. High levels of ZO-3 expression are abrogated in the vicinity of scratch wounds and cell detachment is increased in the absence of ZO-3. These observations strongly suggest that ZO-3 protein plays a role in increasing the adhesive strength of CD epithelia, an event that may rely on several cellular components. These include CycD1, integrins and occludin. In line with our results, CycD1 was previously shown to negatively influence cell adhesion in addition to its key role in regulating cell proliferation.[35,37] Notably, ablation of CycD1 was found to increase matrix adhesion in macrophages and fibroblasts.[35,36] Interestingly, distribution of ZO-3 protein in the kidney described in the present study was very similar to that recently described for occludin.[25] Occludin was previously found to interact with ZOs.[41,42,50] In addition, overexpression of occludin in various cultured cells dramatically increases transepithelial electrical resistance[43,44] and cell adhesiveness.[45] These studies indicate that occludin expressed at TJs may increase cell-cell adhesion. The present study demonstrates good correlation between ZO-3 and occludin abundance and expression at intercellular junctions, increased cell detachment by occludin silencing and decreased occludin abundance by ZO-3 silencing. These data suggest that ZO-3 may increase adhesive strength of CD epithelia in conjunction with occludin, possibly as part of a same complex containing ZO-1. Our data additionally hint that increased cell detachment by ZO-3 silencing may involve integrins. Integrins are heterodimeric adhesion molecules that act as receptors regulating various cellular responses, including migration, proliferation and differentiation.[40] Interaction between integrins and ZO-1 was previously demonstrated and shown to be actively involved in cell migration.[39,51] While ZO-3 silencing did not affect β_1-integrin abundance, it did alter the intracellular distribution of active β_1-integrin, alluding to a diminished ability of integrins to interact with basal lamina.

ZONAB and CycD1 were previously found to play roles in controlled cell proliferation by ZO proteins.[11,16,19,28] Our data show that decreased expression of either ZO-1 or ZO-2 reduced $mCCD_{cl1}$ cell number, increased cell volume and attenuated cell cycle progression. ZO-2 silencing decreased CycD1 abundance and cell cycle progression was similarly affected by either CycD1 or ZO-2 silencing. These observations indicate that ZO-2 silencing reduces $mCCD_{cl1}$ proliferation at least partly by reducing CycD1 expression. How does ZO-1 affect $mCCD_{cl1}$ proliferation? Unlike ZO-2 silencing, ZO-1 silencing increased CycD1 abundance. An increase of nuclear CycD1 can lead to senescent-type cell-cycle arrest.[52–54] However, simultaneous ZO-1 and CycD1 silencing perturbed cell cycle progression to an even greater extent than by either siRNA species acting alone. This indicates that decreased cell cycle progression by siZO-1 does not result from increased nuclear CycD1 abundance. Moreover, ZO-3 silencing, which does not alter cell cycle progression, similarly increased CycD1 nuclear abundance, suggesting that this effect of ZO-1 silencing could indirectly arise from attenuated ZO-3 expression. Elevated nuclear CycD1 localization, however, may have important consequences on cell adhesion, as considered below. On the other hand, altered cell cycling progression by ZO-1 silencing arises at least partly from an increase of nuclear p21 localization since cell cycling was rescued by p21 depletion. ZONAB-long may play a role in this event since its expression is decreased by ZO-1 silencing and since p21 expression and cell cycle progression are similarly affected by silencing of either ZO-1 or ZONAB. Analogous to ZO-1-deficient $mCCD_{cl1}$ cells, depletion of RNA processing factor symplekin decreased proliferation of a subclone of HT-29 cells.[55] This was associated with decreased ZONAB-long, but not ZONAB-short, protein expression in the absence of altered mRNA expression. In addition to enhancing p21 nuclear localization, decreased ZONAB-long expression might affect other factors that delay cell cycle progression. This may involve other inhibitors of the cell cycle and altered transcriptional regulation and/or nucleocytoplasmic shuttling of transcription factors and intracellular signaling components, such as that activated by RhoA via ZO-1/cingulin-containing complexes.[56,57]

Figure 7 (See previous page). Increased cell detachment by ZO-3 depletion relies on a multifactorial process. (**A**) Cells were transfected 1 day after seeding with scrambled siRNA (sc), siRNA against either CycD1 (siCycD1), ZO-3 (siZO-3) or both siCycD1 and siZO-3 and whole cell protein expression was analyzed by Western blot 2 d later (at T2). β-actin was used as a loading control. Quantification of data, shown at right, is represented as fold difference of protein expression over values obtained in cells transfected with scrambled siRNA and is expressed as the mean ± SEM of 3 independent experiments. (**B**) Quantification of cell detachment by flow cytometry of cells transfected as in (A). (**C**) Quantification of cell detachment by flow cytometry of cells transfected with scrambled siRNA (sc), siZO-3, or siRNA against β_1-integrin (siInt) or occludin (siOcc). Data of (**B** and **C**) is represented as fold difference of detached cells over values obtained in cells transfected with scrambled siRNA at T2 and is expressed as the mean ± SEM of 4 independent experiments. (**D**) Western blot of whole-cell ZO-3, β_1-integrin and occludin. β-actin was used as a loading control. Quantification of data is shown at right and is represented as fold difference of protein expression over values obtained at T2 and is expressed as the mean ± SEM of 4 independent experiments. (**E**) Single frame confocal images of β_1-integrin in individual cells. Active β_1-integrin was virtually absent in focal adhesions by ZO-3 silencing. β_1-integrin was also absent in lamellipodium, the mobile edge of cells highlighted in white. (**F**) Western blot of whole-cell ZO-3 and occludin illustrating their parallel increase of expression with cell density. β-actin was used as a loading control. Quantification of data, shown below, is represented as fold difference of protein expression over values obtained 3 d after seeding and is expressed as the mean ± SEM of 3 independent experiments. (**G**) Occludin (green) immunofluorescence in low- and high-density cells. Shown are confocal z-stacks depicting its expression at intercellular junctions in low (D3) and high (D7) density cells. Enlarged single-plane images of Hoechst (blue) or immunofluorescence staining of cells are also shown below. Also shown are double-stained confocal z-stacks of high-density cells scratched 6 h previously depicting both ZO-3 (red) and occludin (green) at the scratch wound and at more distant regions. One of 3 similar experiments is shown. Bar, 10 μm.

All 3 ZO proteins could theoretically localize to the nucleus since they all contain nuclear localization and nuclear export signals.[28,29] In the present study, we provide strong evidence that all 3 ZO proteins accumulate not only at $mCCD_{cl1}$ junctional sites but can also shuttle to the nucleus. Despite our best attempts, we were unable to obtain conclusive data for nuclear expression of any ZO protein by confocal microscopy. Among other factors, this may possibly arise from the incapacity of anti-ZO IgG to recognize epitopes masked by ZO-binding partners, a deterrent resolved by Western blot analysis of nuclear preparations. Data obtained by this approach indicate that ZO-3 nuclear expression dramatically increases with cell confluency. At present, we can only speculate on its implications. Several transcription factors, such as Jun, Fos, AP-1, C/EBP and Yes kinase-associated protein-2 (YAP2) were shown to be actively imported and exported into and from the nucleus when bound to ZO-2.[10,15,58] Possibly, ZO-3 may play a similar shuttling role. Complexes containing ZO-3 and CycD1 were previously identified in cultured colonic epithelial cells.[19] Along with our observation that ZO-3 silencing increases CycD1 nuclear abundance, these data offer the intriguing possibility that ZO-3 may be involved in CycD1 nuclear export in CD principal cells. As indicated by our data and as previously proposed,[35–37] a build-up of nuclear CycD1 may negatively influence cell adhesion.

Some of the observations made in the present study on $mCCD_{cl1}$ cells contrast with previous observations, notably with respect to the influence of ZO-1 on ZONAB and CycD1 activity. MDCK cells overexpressing ZO-1 sequestrate ZONAB at junctional sites.[14] This is associated with reduced entry of cells into S-phase and reduced cell proliferation.[59] In line with this, and similar to $mCCD_{cl1}$ cells (our study) reduced ZONAB expression by RNAi decreases MDCK proliferation.[59] Similar to our observations in $mCCD_{cl1}$ cells, whole-cell abundance and nuclear localization of ZONAB, CycD1 and PCNA decreased with MDCK cell density and ZO-1 was well expressed at junctional sites of confluent cells in both cell lines. On the other hand, anti-ZONAB IgG revealed an immunofluorescent signal at the cell periphery of sparse, but not dense, $mCCD_{cl1}$ cells and cell proliferation was decreased, not increased, by siZO-1. This was accompanied by decreased ZONAB-long and increased CycD1 nuclear expression. While ZONAB silencing in $mCCD_{cl1}$ cells decreased G_1-to-S phase transition it increased CycD1 protein abundance and had no effect on PCNA protein abundance. ZONAB overexpression increased CycD1 abundance in MDCK cells [11] and PCNA abundance in OK and MCF-10A cells.[11,12] These data indicate that CycD1 and PCNA may be differently affected by ZONAB between different cells lines. Like ZO-1, some discrepancies between MDCK and $mCCD_{cl1}$ cells were observed regarding ZO-2. Unlike $mCCD_{cl1}$ cells, Western blot and immunostaining analysis revealed that ZO-2 nuclear expression does not increase but rather decreases with MDCK cell density.[29] We also found that unlike MDCK cells [16,17] decreased $mCCD_{cl1}$ proliferation by siZO-2 is associated with decreased levels of total and nuclear CycD1 protein but not CycD1 mRNA. At least some of these discrepancies may be explained by different experimental approaches used for each study, such as ZO overexpression vs ZO depletion. Additionally, the disparate influence of numerous factors that collectively control cell proliferation may differ between cell lines. This may include differences of activity levels of any one of numerous molecules, including c-Myc, PTEN, SIP1 and p53, that regulate CycD1 transcription.[16,60,62] Post-transcriptional CycD1 processing may also vary between cell lines.

In summary, our results unexpectedly revealed that depletion of either ZO-1 or ZO-2 expression decreases $mCCD_{cl1}$ cell cycle progression while ZO-3 depletion decreases cell adhesion. This leads us to propose a model of how each ZO protein affects kidney CD principal cell proliferation. ZO-2 would increase cell cycle progression partly by increasing CycD1 abundance while ZO-3, which is expressed well after ZO-1, would enhance cell adhesion partly by decreasing nuclear CycD1. ZO-3 may additionally enhance integrin expression at lamellipodium and focal adhesions and occludin expression at intercellular junctions. ZO-1 would play a role in both cellular processes by increasing cell cycle progression, via decreased p21 nuclear localization, and by increasing ZO-3 mRNA translation, thereby also affecting cell adhesion. These data divulge how ZO proteins collectively influence proliferation and adhesion properties of kidney CD principal cells.

Materials and Methods

Antibodies and reagents

The following antibodies were used for Western blot and microscopy analysis: rat anti-ZO-1 (Millipore, NG1853799), rabbit anti-ZO-1 (Invitrogen, 61–7300), rabbit anti-ZO-2 (Invitrogen, 71–1400), rabbit anti-ZO-3 (Invitrogen, 36–4100), rabbit anti-ZONAB (Novex, 40–2800), rabbit anti-CycD1 (Santa Cruz, sc-717), mouse anti-CycD1 (Santa Cruz, sc-450), mouse anti-PCNA (Santa Cruz, sc-56), rabbit anti-p21 (Santa Cruz, sc-397), rabbit anti-calreticulin (Cell Signaling, 12238), rabbit anti-HDAC3 (Cell Signaling, 2632), mouse anti-α-tubulin (Sigma-Aldrich, T9026), mouse anti-β-actin (Sigma-Aldrich, A5441), mouse anti-claudin-4 (Invitrogen, 32–9400), rabbit claudin-8 (Invitrogen, 40–0700Z), mouse anti-occludin (Invitrogen, 33–1500), rabbit anti-β1-integrin (Abcam, 52971) and rat anti-β1-integrin (9EG7) (BD Biosciences, 553715). Secondary antibodies used were as follows: Horseradish peroxidase (HRP)-conjugated goat anti-mouse (BD, 554002), HRP-conjugated goat anti-rabbit (BD, 554021), HRP-conjugated goat anti-rat (Invitrogen, 629520), goat anti-mouse Alexa Fluor 488 (Invitrogen, A-11017), goat anti-rabbit Alexa Fluor 488 (Invitrogen, A-11070), goat anti-rat Alexa Fluor 488 (Jackson ImmunoResearch Laboratories, 112-545-003) goat anti-rabbit CY3 (Jackson ImmunoResearch Laboratories, 111-165-003), goat anti-mouse CY3 (Jackson ImmunoResearch Laboratories, 115-166-003), goat anti-rat Alexa Fluor 546 (Invitrogen, A11081).

Cell culture and transfection

$mCCD_{cl1}$ cells[26] were cultured with medium previously described. [63] Cells were transfected one day after seeding with

INTERFERin (Polyplus-transfection, 409-10) in the presence of 10 nM siRNA according to the manufacturer's instructions. siRNA sequences are depicted in **Table 1**.

Cell number and confluency analysis

For analysis of $mCCD_{cl1}$ growth curves, confluent cells (with domes) that reached a growth-arrested state were trypsinized and seeded (30,000 cells/well) in 12-well plates. Cell number at day 3–9 was counted with a hemocytometer. Images were taken prior to counting cells with an inverted phase contrast microscope and cell size was analyzed by ImageJ.

To measure the number and confluency of siRNA-transfected cells, we used the ImageXpress Micro Widefield High Content Screening System (Molecular Devices). Cells (30,000 cells/well) were seeded on 12-well plates and transfected with siRNA 24 h later. On the day of experiment, cells were incubated with Hoechst 33342 (1:2000, Invitrogen, H1399) for 5 min to label nuclei and 85% of each well surface was imaged by ImageXpress. A set of transmitted light images and corresponding fluorescent images of labeled nuclei were acquired. Transmitted light and fluorescent image overlay was done by MetaXpress software (Molecular Devices). Cell number was analyzed by MetaXpress software by counting nuclei. For cells transfected for 6 days, cells were counted with a Tali® Image-Based Cytometer (Invitrogen). Cell confluence of each experimental point was calculated by dividing the number of pixels corresponding to cells over the total number of pixels contained in the entire image using the ImageJ Color Threshold plugin.

Cell volume analysis

Confluent cells (with domes) that reached a growth-arrested state were trypsinized and seeded (60,000 cells/well) in 6-well plates and transfected with siRNA 24 h later. For each indicated time point, cells were trypsinized to obtain single cell suspensions, and cell volume was measured by CASY1 (Schärfe System, Germany). The principle of volume measurement is based on a combination of an established particle measurement technique, the "resistance measuring principle," and the pulse area analysis signal-processing technique.[64]

Cell cycle analysis

Cells were washed in PBS (Ca^{2+}/Mg^{2+}–free) and trypsinized to obtain single cell suspensions. Cells were then fixed in 5 ml 70% ice-cold ethanol. Fixed cells were incubated in 0.02 mg/ml propidium iodide (Sigma-Aldrich, P4864), 0.2 mg/ml RNase A (Roche, 109169), and 0.05% Triton X-100 for 30 min at 37°C. Flow cytometry measurements were performed by an Accuri C6 apparatus (Becton Dickinson) and data was analyzed with FlowJo software (Tree Star).

Cell death analysis

Attached cells were trypsinized, spun at 200 g for 10 min, washed with ice-cold PBS, resuspended in binding buffer (10 mM HEPES, 140 mM NaCl, 2.5 mM CaCl2, pH 7.4) at 1×10^6 cells/ml and incubated with APC-conjugated Annexin V (5 μl /100 μl cell suspension, BD PharMingen, 550475) at room temperature for 15 min. 400 μl of binding buffer containing 1 μl propidium iodide (1 mg/ml, Sigma-Aldrich, P4864) was then added and incubated on ice for 5 min. Cells were analyzed using Accuri C6 and CFlow software (Becton Dickinson).

Cell detachment analysis

Cells cultured in 6-well plates were transfected with scrambled siRNA or siRNA against target genes. To quantify cell detachment, cells were incubated in 2 ml fresh medium 2 d post-transfection for 16 hours. Suspensions were collected and equal volumes (200 μl) were analyzed using Accuri C6 and CFlow software (Becton Dickinson). Detached cells were identified according to their FSC/SSC value.

Fractionation of membrane/cytoplasmic and nuclear proteins

Cells were scrapped off, spun at 2000 rpm, resuspended in buffer A (10 mM HEPES-KOH, pH 7.9, 50 mM NaCl, 0.5 mM Sucrose, 0.1 mM EDTA, 0.5% Triton X-100, 100 mM NaF and 1 mM PMSF) on ice for 5 min and spun at 1000 rpm for 5 min. The supernatant, corresponding to membrane/cytosolic extract, was collected, spun at 14,000 rpm for 15 min for purification and collected a second time. The pellet was washed in buffer B (10 mM HEPES-KOH, pH 7.9, 10 mM KCl, 0.1 mM EDTA, 0.1 mM EGTA and 1 mM PMSF) and spun at 1000 rpm for 5 min. This step was repeated 3 times. The pellet was then resuspended in buffer C (10 mM HEPES-KOH, pH 7.9, 500 mM NaCl, 0.1 mM EDTA, 0.1 mM EGTA, 0.1% NP-40, 1 mM PMSF), vigorously vortexed every 5 min on ice for 30 min and spun at 14,000 rpm. The supernatant, corresponding to nuclear extract, was then collected. Equal amounts of membrance/cytoplasmic and nuclear protein were loaded on gels for Western blot analysis.

Immunofluorescence

Cells seeded on glass coverslips were fixed in methanol for 10 min at -20°C or in 4% paraformaldehyde (PFA) for 20 min at room temperature. Cells were blocked with 3% bovine serum albumin (BSA) for 30 min. PFA-fixed cells were permeabilized in 0.1% Triton X-100 for 3 min. Primary antibodies were detected with Alexa488 and/or CY3-labeled secondary antibodies in PBS with 0.1% BSA and then mounted in SlowFade mounting medium (Invitrogen, S36936). Antibodies were applied at the following dilutions: rat anti-ZO-1 (1:500), rabbit anti-ZO-1 (1:500), ZO-2 (1:500), ZO-3 (1:500), ZONAB (1:500), rabbit anti-CycD1 (1:500), mouse anti-CycD1 (1:500), claudin-4 (1:500), claudin-8 (1:500), occludin (1:500), PCNA (1:1000) and rat anti-β1-integrin (1:2500). Secondary antibodies were applied at a 1:1000 dilution. Fluorescence images were acquired by confocal laser scanning microscopy using a LSM700 confocal microscope (Zeiss) and Zen 2010b image analysis software (Zeiss). Image quantitation was performed using ImageJ.

Real-time PCR analysis

RNA extraction, reverse transcription and real-time PCR analysis was performed as previously described.[65] Primers used are depicted in **Table 1**.

Western blot analysis

Preparation of cell lysates was performed as previously described[66] and equal amounts of protein were separated by NuPage 4–12% Bis-Tris gel (Invitrogen), transferred to polyvinylidene difluoride membranes (Immobilon-P, Millipore) and detected using rat anti-ZO-1 (1:1000), rabbit anti-ZO-1 (1:1000), ZO-2 (1:1000), ZO-3 (1:500), ZONAB (1:1000), rabbit anti-CycD1 (1:500), mouse anti-CycD1 (1:500), PCNA (1:1000), p21 (1:1000), occludin (1:500), calreticulin (1:1000), HDAC3 (1:1000), rabbit anti-β1-integrin (1:500), α-tubulin (1:5000) or β-actin (1:10000). Bands were quantified using Photoshop (Adobe Systems). Experiments were repeated at least 3 times with consistent results.

Isolation of rat kidney tubules

Sprague-Dawley rats weighing 200–250 g were anesthetized with 5 mg/100 g intraperitoneal pentobarbital, and the left kidney was perfused via the abdominal aorta with incubation solution (120 mM NaCl, 5 mM KCl, 4 mM $NaHCO_3$, 1 mM $CaCl_2$, 1 mM $MgSO_4$, 0.2 mM NaH_2PO_4, 0.15 mM Na_2HPO_4, 5 mM glucose, 10 mM lactate, 1 mM pyruvate, 4 mM essential and nonessential amino acids, 0.03 mM vitamins, 20 mM HEPES, and 0.1% BSA [pH 7.45]) containing 5% (vol/vol) of collagenase (Blendzyme 2; Roche), removed, sliced into small pyramids and incubated for 20 min at 30°C in oxygenated (95% O_2 and 5% CO_2) incubation solution containing 1% (vol/vol) of collagenase. Single cortical collecting ducts, medullary collecting ducts and S1 proximal tubules were isolated by microdissection in ice-cold oxygenated incubation solution and stored at 4°C until used. Each experimental group was constituted by pools of 50 tubules from the same rat. All animal experiments were approved by the Institutional Ethical Committee of Animal Care in Geneva and Cantonal authorities.

Rat kidney immunolabeling

Immunolabeling was performed on 4% paraformaldehyde-fixed and paraffin-embedded, 5 μm thick kidney sections using the TEG-buffer (10 mM Tris, 0.5 mM EGTA, pH 9) microwave-based antigen retrieval technique and using the EnVision Flex kit (Agilent Technologies). Antibodies were applied at the following dilutions: rat anti-ZO-1 (1:1000), rabbit anti-ZO-2 (1:1000) and rabbit anti-ZO-3 (1:500). Secondary antibodies were applied at a 1:1000 dilution. Confocal imaging and image analysis was performed as described above.

Statistical analysis

Results are given as the mean ± SEM from n independent experiments. All statistical analyses were performed using Origin 8.1 (OriginLab). Western blot analysis was performed by Student's t-test. Cell detachment analysis was performed by one-way ANOVA and post-hoc Dunnett's multiple comparison test. One-way ANOVA and post-hoc Tukey's test was used in all other instances. *$p \leq 0.05$ was considered to be significant.

Disclosure of Potential Conflicts of Interest

No potential conflicts of interest were disclosed.

Acknowledgments

We thank Sandra Citi and Paula Nunes for critical reading of the manuscript and helpful suggestions.

Funding

This work was supported by a Swiss National Science Foundation Grant 31003A_138408/1 and grants from the Fondation Schmidheiny and the National Center of Competence in Research (NCCR) Kidney.CH to U.H.

References

1. Steed E, Balda MS, Matter K. Dynamics and functions of tight junctions. Trends Cell Biol 2010; 20:142-9; PMID:20061152; http://dx.doi.org/10.1016/j.tcb.2009.12.002
2. Amasheh S, Fromm M, Gunzel D. Claudins of intestine and nephron - a correlation of molecular tight junction structure and barrier function. Acta Physiol (Oxf) 2011; 201:133-40; PMID:20518752; http://dx.doi.org/10.1111/j.1748-1716.2010.02148.x
3. Van Itallie CM, Anderson JM. Claudins and epithelial paracellular transport. Ann Rev Physiol 2006; 68:403-29; PMID:16460278; http://dx.doi.org/10.1146/annurev.physiol.68.040104.131404
4. Will C, Fromm M, Muller D. Claudin tight junction proteins: novel aspects in paracellular transport. Peritoneal dialysis international : J Int Soc Peritoneal Dial 2008; 28:577-84.
5. Bauer H, Zweimueller-Mayer J, Steinbacher P, Lametschwandtner A, Bauer HC. The dual role of zonula occludens (ZO) proteins. J Biomed Biotechnol 2010; 2010:402593.
6. Balda MS, Matter K. Epithelial cell adhesion and the regulation of gene expression. Trends Cell Biol 2003; 13:310-8; PMID:12791297; http://dx.doi.org/10.1016/S0962-8924(03)00105-3
7. Matter K, Balda MS. Signalling to and from tight junctions. Nat Rev Mol Cell Biol 2003; 4:225-36; PMID:12612641; http://dx.doi.org/10.1038/nrm1055
8. Gonzalez-Mariscal L, Tapia R, Chamorro D. Crosstalk of tight junction components with signaling pathways. Biochimica Et Biophysica Acta 2008; 1778:729-56; PMID:17950242; http://dx.doi.org/10.1016/j.bbamem.2007.08.018
9. Balda MS, Matter K. Tight junctions and the regulation of gene expression. BBA-Biomembranes 2009; 1788:761-7; PMID:19121284; http://dx.doi.org/10.1016/j.bbamem.2008.11.024
10. Matter K, Balda MS. Epithelial tight junctions, gene expression and nucleo-junctional interplay. J Cell Sci 2007; 120:1505-11; PMID:17452622; http://dx.doi.org/10.1242/jcs.005975
11. Sourisseau T, Georgiadis A, Tsapara A, Ali RR, Pestell R, Matter K, Balda MS. Regulation of PCNA and cyclin D1 expression and epithelial morphogenesis by the ZO-1-regulated transcription factor ZONAB/DbpA. Mol Cell Biol 2006; 26:2387-98; PMID:16508013; http://dx.doi.org/10.1128/MCB.26.6.2387-2398.2006
12. Lima WR, Parreira KS, Devuyst O, Caplanusi A, N'Kuli F, Marien B, Van Der Smissen P, Alves PM, Verroust P, Christensen EI, et al. ZONAB promotes proliferation and represses differentiation of proximal tubule epithelial cells. J Am Soc Nephrol: JASN 2010; 21:478-88; PMID:20133480; http://dx.doi.org/10.1681/ASN.2009070698
13. Sherr CJ. D-type cyclins. Trends Biochem Sci 1995; 20:187-90; PMID:7610482; http://dx.doi.org/10.1016/S0968-0004(00)89005-2
14. Balda MS, Matter K. The tight junction protein ZO-1 and an interacting transcription factor regulate ErbB-2 expression. EMBO J 2000; 19:2024-33; PMID:10790369; http://dx.doi.org/10.1093/emboj/19.9.2024
15. Betanzos A, Huerta M, Lopez-Bayghen E, Azuara E, Amerena J, Gonzalez-Mariscal L. The tight junction

protein ZO-2 associates with Jun, Fos and C/EBP transcription factors in epithelial cells. Exp Cell Res 2004; 292:51-66; PMID:14720506; http://dx.doi.org/10.1016/j.yexcr.2003.08.007

16. Huerta M, Munoz R, Tapia R, Soto-Reyes E, Ramirez L, Recillas-Targa F, González-Mariscal L, López-Bayghen E. Cyclin D1 is transcriptionally down-regulated by ZO-2 via an E box and the transcription factor c-Myc. Mol Biol Cell 2007; 18:4826-36; PMID:17881732; http://dx.doi.org/10.1091/mbc.E07-02-0109
17. Tapia R, Huerta M, Islas S, Avila-Flores A, Lopez-Bayghen E, Weiske J, Huber O, González-Mariscal L. Zona occludens-2 inhibits cyclin D1 expression and cell proliferation and exhibits changes in localization along the cell cycle. Mol Biol Cell 2009; 20:1102-17; PMID:19056685; http://dx.doi.org/10.1091/mbc.E08-03-0277
18. Inoko A, Itoh M, Tamura A, Matsuda M, Furuse M, Tsukita S. Expression and distribution of ZO-3, a tight junction MAGUK protein, in mouse tissues. Genes Cells: Dev Mol Cell Mech 2003; 8:837-45.
19. Capaldo CT, Koch S, Kwon M, Laur O, Parkos CA, Nusrat A. Tight function zonula occludens-3 regulates cyclin D1-dependent cell proliferation. Mol Biol Cell 2011; 22:1677-85; PMID:21411630; http://dx.doi.org/10.1091/mbc.E10-08-0677
20. Adachi M, Inoko A, Hata M, Furuse K, Umeda K, Itoh M, Tsukita S. Normal establishment of epithelial tight junctions in mice and cultured cells lacking expression of ZO-3, a tight-junction MAGUK protein. Mol Cell Biol 2006; 26:9003-15; PMID:17000770; http://dx.doi.org/10.1128/MCB.01811-05
21. Xu J, Kausalya PJ, Phua DC, Ali SM, Hossain Z, Hunziker W. Early embryonic lethality of mice lacking ZO-2, but Not ZO-3, reveals critical and nonredundant roles for individual zonula occludens proteins in mammalian development. Mol Cell Biol 2008; 28:1669-78; PMID:18172007; http://dx.doi.org/10.1128/MCB.00891-07
22. Hou J. Regulation of paracellular transport in the distal nephron. Curr Opin Nephrol Hypertens 2012; 21:547-51; PMID:22691877; http://dx.doi.org/10.1097/MNH.0b013e328355cb47
23. Hou J, Rajagopal M, Yu AS. Claudins and the kidney. Ann Rev Physiol 2013; 75:479-501; PMID:23140368; http://dx.doi.org/10.1146/annurev-physiol-030212-183705
24. Gonzalez-Mariscal L, Namorado MC, Martin D, Luna J, Alarcon L, Islas S, Valencia L, Muriel P, Ponce L, Reyes JL. Tight junction proteins ZO-1, ZO-2, and occludin along isolated renal tubules. Kidney Int 2000; 57:2386-402; PMID:10844608; http://dx.doi.org/10.1046/j.1523-1755.2000.00098.x
25. Lee SY, Shin JA, Kwon HM, Weiner ID, Han KH. Renal ischemia-reperfusion injury causes intercalated cell-specific disruption of occludin in the collecting duct. Histochem Cell Biol 2011; 136:637-47; PMID:22048282; http://dx.doi.org/10.1007/s00418-011-0881-4
26. Gaeggeler HP, Gonzalez-Rodriguez E, Jaeger NF, Loffing-Cueni D, Norregaard R, Loffing J, Horisberger JD, Rossier BC. Mineralocorticoid versus glucocorticoid receptor occupancy mediating aldosterone-stimulated sodium transport in a novel renal cell line. J Am Soc Nephrol: JASN 2005; 16:878-91; PMID:15743993; http://dx.doi.org/10.1681/ASN.2004121110
27. Gaeggeler HP, Guillod Y, Loffing-Cueni D, Loffing J, Rossier BC. Vasopressin-dependent coupling between sodium transport and water flow in a mouse cortical collecting duct cell line. Kidney Int 2011; 79:843-52; PMID:21178974; http://dx.doi.org/10.1038/ki.2010.486
28. Gonzalez-Mariscal L, Islas S, Contreras RG, Garcia-Villegas MR, Betanzos A, Vega J, Diaz-Quiñónez A, Martín-Orozco N, Ortiz-Navarrete V, Cereijido M, et al. Molecular characterization of the tight junction protein ZO-1 in MDCK cells. Exp Cell Res 1999; 248:97-109; PMID:10094817; http://dx.doi.org/10.1006/excr.1999.4392
29. Islas S, Vega J, Ponce L, Gonzalez-Mariscal L. Nuclear localization of the tight junction protein ZO-2 in epithelial cells. Exp Cell Res 2002; 274:138-48; PMID:11855865; http://dx.doi.org/10.1006/excr.2001.5457
30. Roth I, Leroy V, Kwon HM, Martin PY, Feraille E, Hasler U. Osmoprotective transcription factor NFAT5/TonEBP modulates nuclear factor-kappaB activity. Mol Biol Cell 2010; 21:3459-74; PMID:20685965; http://dx.doi.org/10.1091/mbc.E10-02-0133
31. Misfeldt DS, Hamamoto ST, Pitelka DR. Transepithelial transport in cell culture. Proc Natl Acad Sci USA 1976; 73:1212-6; PMID:1063404; http://dx.doi.org/10.1073/pnas.73.4.1212
32. Cereijido M, Robbins ES, Dolan WJ, Rotunno CA, Sabatini DD. Polarized monolayers formed by epithelial cells on a permeable and translucent support. J Cell Biol 1978; 77:853-80; PMID:567227; http://dx.doi.org/10.1083/jcb.77.3.853
33. Diehl JA, Cheng M, Roussel MF, Sherr CJ. Glycogen synthase kinase-3beta regulates cyclin D1 proteolysis and subcellular localization. Genes Dev 1998; 12:3499-511; http://dx.doi.org/10.1101/gad.12.22.3499
34. Guo Y, Yang K, Harwalkar J, Nye JM, Mason DR, Garrett MD, Hitomi M, Stacey DW. Phosphorylation of cyclin D1 at Thr 286 during S phase leads to its proteasomal degradation and allows efficient DNA synthesis. Oncogene 2005; 24:2599-612; PMID:15735756; http://dx.doi.org/10.1038/sj.onc.1208326
35. Neumeister P, Pixley FJ, Xiong Y, Xie H, Wu K, Ashton A, Cammer M, Chan A, Symons M, Stanley ER, et al. Cyclin D1 governs adhesion and motility of macrophages. Mol Biol Cell 2003; 14:2005-15; PMID:12802071; http://dx.doi.org/10.1091/mbc.02-07-0102
36. Li Z, Wang C, Jiao X, Lu Y, Fu M, Quong AA, Dye C, Yang J, Dai M, Ju X, et al. Cyclin D1 regulates cellular migration through the inhibition of thrombospondin 1 and ROCK signaling. Mol Cell Biol 2006; 26:4240-56; PMID:16705174; http://dx.doi.org/10.1128/MCB.02124-05
37. Fernandez-Hernandez R, Rafel M, Fuste NP, Aguayo RS, Casanova JM, Egea J, Ferrezuelo F, Garí E. Cyclin D1 localizes in the cytoplasm of keratinocytes during skin differentiation and regulates cell-matrix adhesion. Cell Cycle 2013; 12:2510-7; PMID:23839032; http://dx.doi.org/10.4161/cc.25590
38. Akhtar N, Streuli CH. An integrin-ILK-microtubule network orients cell polarity and lumen formation in glandular epithelium. Nat Cell Biol 2013; 15:17-27; PMID:23263281; http://dx.doi.org/10.1038/ncb2646
39. Tuomi S, Mai A, Nevo J, Laine JO, Vilkki V, Ohman TJ, Gahmberg CG, Parker PJ, Ivaska J. PKCepsilon regulation of an alpha5 integrin-ZO-1 complex controls lamellae formation in migrating cancer cells. Sci Signaling 2009; 2:ra32; PMID:19567915; http://dx.doi.org/10.1126/scisignal.2000135
40. Hynes RO. Integrins: bidirectional, allosteric signaling machines. Cell 2002; 110:673-87; PMID:12297042; http://dx.doi.org/10.1016/S0092-8674(02)00971-6
41. Haskins J, Gu L, Wittchen ES, Hibbard J, Stevenson BR. ZO-3, a novel member of the MAGUK protein family found at the tight junction, interacts with ZO-1 and occludin. J Cell Biol 1998; 141:199-208; PMID:9531559; http://dx.doi.org/10.1083/jcb.141.1.199
42. Peng BH, White MA, Campbell GA, Robert JJ, Lee JC, Sutton RB. Crystallization and preliminary X-ray diffraction of the ZO-binding domain of human occludin. Acta Crystallogr Sec F, Struct Biol Crystallization Commun 2005; 61:369-71; PMID:16511043; http://dx.doi.org/10.1107/S1744309105007475
43. Balda MS, Whitney JA, Flores C, Gonzalez S, Cereijido M, Matter K. Functional dissociation of paracellular permeability and transepithelial electrical resistance and disruption of the apical-basolateral intramembrane diffusion barrier by expression of a mutant tight junction membrane protein. J Cell Biol 1996; 134:1031-49; PMID:8769425; http://dx.doi.org/10.1083/jcb.134.4.1031
44. McCarthy KM, Skare IB, Stankewich MC, Furuse M, Tsukita S, Rogers RA, Lynch RD, Schneeberger EE. Occludin is a functional component of the tight junction. J Cell Sci 1996; 109 (Pt 9):2287-98; PMID:8886979
45. Van Itallie CM, Anderson JM. Occludin confers adhesiveness when expressed in fibroblasts. J Cell Sci 1997; 110 (Pt 9):1113-21; PMID:9175707
46. Rachow S, Zorn-Kruppa M, Ohnemus U, Kirschner N, Vidal-y-Sy S, von den Driesch P, Börnchen C, Eberle J, Mildner M, Vettorazzi E, et al. Occludin is involved in adhesion, apoptosis, differentiation and Ca^{2+}-homeostasis of human keratinocytes: implications for tumorigenesis. PLoS One 2013; 8:e55116; PMID:23390516; http://dx.doi.org/10.1371/journal.pone.0055116
47. Wittchen ES, Haskins J, Stevenson BR. Protein interactions at the tight junction. Actin has multiple binding partners, and ZO-1 forms independent complexes with ZO-2 and ZO-3. J Biol Chem 1999; 274:35179-85; PMID:10575001; http://dx.doi.org/10.1074/jbc.274.49.35179
48. Fanning AS, Van Itallie CM, Anderson JM. Zonula occludens-1 and -2 regulate apical cell structure and the zonula adherens cytoskeleton in polarized epithelia. Mol Biol Cell 2012; 23:577-90; PMID:22190737; http://dx.doi.org/10.1091/mbc.E11-09-0791
49. Rodgers LS, Beam MT, Anderson JM, Fanning AS. Epithelial barrier assembly requires coordinated activity of multiple domains of the tight junction protein ZO-1. J Cell Sci 2013; 126:1565-75; PMID:23418357; http://dx.doi.org/10.1242/jcs.113399
50. Furuse M, Itoh M, Hirase T, Nagafuchi A, Yonemura S, Tsukita S, Tsukita S. Direct association of occludin with ZO-1 and its possible involvement in the localization of occludin at tight junctions. J Cell Biol 1994; 127:1617-26; PMID:7798316; http://dx.doi.org/10.1083/jcb.127.6.1617
51. Huo L, Wen W, Wang R, Kam C, Xia J, Feng W, Zhang M. Cdc42-dependent formation of the ZO-1/MRCKbeta complex at the leading edge controls cell migration. EMBO J 2011; 30:665-78; PMID:21240187; http://dx.doi.org/10.1038/emboj.2010.353
52. Leontieva OV, Demidenko ZN, Blagosklonny MV. MEK drives cyclin D1 hyperelevation during geroconversion. Cell Death Differ 2013; 20:1241-9; PMID:23852369; http://dx.doi.org/10.1038/cdd.2013.86
53. Leontieva OV, Lenzo F, Demidenko ZN, Blagosklonny MV. Hyper-mitogenic drive coexists with mitotic incompetence in senescent cells. Cell Cycle 2012; 11:4642-9; PMID:23187803; http://dx.doi.org/10.4161/cc.22937
54. Malumbres M, Perez De Castro I, Hernandez MI, Jimenez M, Corral T, Pellicer A. Cellular response to oncogenic ras involves induction of the Cdk4 and Cdk6 inhibitor p15(INK4b). Mol Cell Biol 2000; 20:2915-25; PMID:10733595; http://dx.doi.org/10.1128/MCB.20.8.2915-2925.2000
55. Kavanagh E, Buchert M, Tsapara A, Choquet A, Balda MS, Hollande F, Matter K. Functional interaction between the ZO-1-interacting transcription factor ZONAB/DbpA and the RNA processing factor symplekin. J Cell Sci 2006; 119:5098-105;

PMID:17158914; http://dx.doi.org/10.1242/jcs.03297
56. D'Atri F, Nadalutti F, Citi S. Evidence for a functional interaction between cingulin and ZO-1 in cultured cells. J Biol Chem 2002; 277:27757-64; PMID:12023291; http://dx.doi.org/10.1074/jbc.M203717200
57. Guillemot L, Citi S. Cingulin regulates claudin-2 expression and cell proliferation through the small GTPase RhoA. Mol Biol Cell 2006; 17:3569-77; PMID:16723500; http://dx.doi.org/10.1091/mbc.E06-02-0122
58. Oka T, Remue E, Meerschaert K, Vanloo B, Boucherie C, Gfeller D, Bader GD, Sidhu SS, Vandekerckhove J, Gettemans J, et al. Functional complexes between YAP2 and ZO-2 are PDZ domain-dependent, and regulate YAP2 nuclear localization and signalling. Biochem J 2010; 432:461-72; PMID:20868367; http://dx.doi.org/10.1042/BJ20100870
59. Balda MS, Garrett MD, Matter K. The ZO-1-associated Y-box factor ZONAB regulates epithelial cell proliferation and cell density. J Cell Biol 2003; 160:423-32; PMID:12566432; http://dx.doi.org/10.1083/jcb.200210020
60. Chung JH, Ostrowski MC, Romigh T, Minaguchi T, Waite KA, Eng C. The ERK1/2 pathway modulates nuclear PTEN-mediated cell cycle arrest by cyclin D1 transcriptional regulation. Hu Mol Genet 2006; 15:2553-9; PMID:16849370; http://dx.doi.org/10.1093/hmg/ddl177
61. Mejlvang J, Kriajevska M, Vandewalle C, Chernova T, Sayan AE, Berx G, Mellon JK, Tulchinsky E. Direct repression of cyclin D1 by SIP1 attenuates cell cycle progression in cells undergoing an epithelial mesenchymal transition. Mol Biol Cell 2007; 18:4615-24; PMID:17855508; http://dx.doi.org/10.1091/mbc.E07-05-0406
62. Rocha S, Martin AM, Meek DW, Perkins ND. p53 represses cyclin D1 transcription through down regulation of Bcl-3 and inducing increased association of the p52 NF-kappaB subunit with histone deacetylase 1. Mol Cell Biol 2003; 23:4713-27; PMID:12808109; http://dx.doi.org/10.1128/MCB.23.13.4713-4727.2003
63. Montesano R, Ghzili H, Carrozzino F, Rossier BC, Feraille E. cAMP-dependent chloride secretion mediates tubule enlargement and cyst formation by cultured mammalian collecting duct cells. Am J Physiol Renal Physiol 2009; 296:F446-57; PMID:19052103
64. Behmanesh S, Kempski O. Mechanisms of endothelial cell swelling from lactacidosis studied in vitro. Am J Physiol Heart Circ Physiol 2000; 279:H1512-7; PMID:11009435
65. Feraille E, Dizin E, Roth I, Derouette JP, Szanto I, Martin PY, de Seigneux S, Hasler U. NADPH Oxidase 4 Deficiency Reduces Aquaporin-2 mRNA Expression in Cultured Renal Collecting Duct Principal Cells via Increased PDE3 and PDE4 Activity. PLoS One 2014; 9:e87239; PMID:24466344; http://dx.doi.org/10.1371/journal.pone.0087239
66. Hasler U, Vinciguerra M, Vandewalle A, Martin P-Y, Feraille E. Dual Effects of Hypertonicity on Aquaporin-2 Expression in Cultured Renal Collecting Duct Principal Cells. J Am Soc Nephrol: JASN 2005; 16:1571-82; PMID:15843469; http://dx.doi.org/10.1681/ASN.2004110930